



Universidade do Porto

**FEUP** Faculdade de  
Engenharia

**Development of a Pilot Installation to Prepare Hydroxyapatite**

**Desenvolvimento de uma Instalação Piloto para a Preparação de Hidroxiapatite**

Carlos Manuel Fernandes Gonçalves

Licenciado em Engenharia Química pela Universidade do Porto

Dissertação submetida para satisfação parcial dos requisitos do grau de mestre em  
Engenharia Biomédica

Dissertação realizada sob a supervisão de:

Professor José Domingos da Silva Santos e

Doutora Cláudia Manuela da Cunha Ferreira Botelho

Porto, Novembro de 2009

Aos meus pais

“Não é a força mas a constância dos bons  
resultados que conduz os homens à felicidade.”

Friedrich Nietzsche

## Resumo

A hidroxiapatite é quimicamente semelhante à fase mineral do osso e dos tecidos rígidos nos mamíferos. É um dos poucos materiais classificado como bioactivo, o que significa que estimula o crescimento ósseo e a osteointegração quando utilizado em diversas aplicações, nomeadamente ortopédicas, odontológicas e maxilo-faciais.

A preparação de hidroxiapatite (HA),  $[Ca_{10}(PO_4)_6(OH)_2]$ , com determinadas características de morfologia, estequiometria, cristalinidade e distribuição do tamanho dos cristais, é importante na biomedicina e na ciência dos materiais. As apatites biológicas não são estequiométricas e apresentam diversos tamanhos; nanométrico no osso e na dentina e micrométrico no esmalte. A HA sintética é normalmente utilizada na preparação de biocerâmicos e compósitos cerâmicos ou poliméricos para aplicações na área da ortopedia, implantologia, medicina dentária e cirurgia maxilofacial.

O principal objectivo deste projecto foi o desenvolvimento de um biorreactor que permitisse a preparação de 500g de HA utilizando a via de precipitação húmida com hidróxido de cálcio e ácido ortofosfórico como reagentes, em apenas 5 horas, controlando vários parâmetros de processo tais como: temperatura, pH, velocidade de adição de reagentes e velocidade de agitação.

A primeira parte do trabalho consistiu na concepção e montagem do biorreactor piloto. Todos os equipamentos e diagrama de processo foram desenhados e dimensionados de forma a criar um sistema com todas as condições de segurança e operacionalidade e cumprindo as regras de funcionamento em condições GMP – “*Good Manufacturing Production*”.

A segunda parte do trabalho foi dedicada à avaliação do sistema concebido, começando por preparar pequenas quantidades de HA e alterando a velocidade de adição de ácido ortofosfórico com o objectivo de preparar grandes quantidades num curto período de tempo.

Os resultados obtidos mostraram que a instalação concebida permite preparar 500g de HA em 5 horas, com as características estabelecidas pela Organização Internacional para a Standardização (ISO) para o uso de HA em medicina.

## Abstract

Hydroxyapatite is chemically similar to the mineral phase of bone and hard tissues in mammals. It is one of the few materials that is classified as bioactive, meaning that it will support bone ingrowth and osteointegration when used in several medical applications, such as: orthopaedics, dental and maxillofacial applications.

The preparation of hydroxyapatite (HA),  $[\text{Ca}_{10}(\text{PO}_4)_6(\text{OH})_2]$ , with given characteristics of morphology, stoichiometry, crystallinity and crystal size distribution is important in biomedicine and materials science. Biological apatites are nonstoichiometric and have a nanometric size in bone and dentin and micrometric size in enamel. Synthetic HA powders are normally used to prepare bioceramics and polymer or ceramic composites for orthopaedics, implantology, dental and maxillofacial surgery.

The aim of the present project was to develop a bioreactor to prepare HA using a wet precipitation method with calcium hydroxide and ortho-phosphoric acid as reagents. It was aimed to prepare 500g of HA in 5 hours with reproducible characteristics, therefore the process parameters such as temperature, pH, reagent addition rate and stir speed were controlled and constantly monitored.

The first part of the work was to design and assemble a pilot bioreactor for the preparation of phase pure HA. Calculations were performed in order to select the correct equipments and designed a system with all the security and operable conditions, according to GMP conditions (Good Manufacturing Production).

The second part was dedicated to evaluate the pilot installation through the preparation of different amounts of HA. The first experiments carried out started with the preparation of small quantities of HA with a variable rate of  $\text{H}_3\text{PO}_4$  addition, in order to prepare larger quantities of HA in a short period of time.

The results obtained showed that the present installation is able to prepare 500g of HA in 5 hours, with the characteristics established by the International Organization for Standardization (ISO) for the use of HA in medicine.

## **Acknowledgements**

I am thankful to my supervisors Professor José Domingos Santos and Dr. Cláudia Botelho for all the availability and help.

My thanks to Marta Laranjeira for all the help and to Sofia Meireles for the patience and partnership on the laboratory work.

A special thanks to Sofia Ferreira for their friendship, trust and encouragement that stimulated me to finish this thesis.

I also want to thank my parents and my sister for the confidence and support given.

# Contents

<b>Chapter 1 – General Introduction.....</b>	<b>9</b>
1 – Overview.....	10
2 - The Bone.....	11
3 - Bone Graft Substitutes.....	13
4 - Bone Tissue Engineering.....	15
5 – Biomaterials.....	18
6 – Hydroxyapatite.....	21
6.1 – HA properties.....	21
6.2 – Applications.....	23
6.3 - Rules for Synthetic Hydroxyapatite Biomedical Application.....	24
6.4 - Preparation Methods.....	25
6.4.1 - Dry Method.....	25
6.4.2 - Hydrothermal Method.....	25
6.4.3 - Alkoxide Method.....	26
6.4.4 - Flux Method.....	26
6.4.5 – Sol-Gel Method.....	27
6.4.6 - Wet Method.....	27
7 – Chemical Reactors and Surrounding Systems.....	28
7.1 – Chemical Reactors.....	29
7.2 – Water Purification.....	30
7.3 – Filtration.....	31
<b>Chapter 2 – Design and Project Description.....</b>	<b>32</b>
1 – Introduction.....	33
2 – Process Diagram.....	34
3 - Water Purification System.....	35
4 - Reaction System.....	35
5 - pH Control System.....	36
6 - Filtration and Vacuum Systems.....	37
7 - Powder Preparation and Sintering.....	37

<b>Chapter 3 – Experimental Procedures</b> .....	39
1 – Introduction.....	40
2 – Evaluation of pH Levels .....	41
3 - Experiments to achieve 500g of HA according to ISO 13779.....	41
4 - Sample Characterisation .....	44
<b>Results</b> .....	46
A – Evaluation of pH Levels .....	47
B – Preparation of HA.....	47
C - Evaluation of functional groups using FTIR analyses.....	52
D – Ca/P and heavy metals determination.....	56
E – HA reproducibility.....	56
<b>Discussion and Conclusions</b> .....	61
Discussion.....	62
Conclusions.....	71
<b>References</b> .....	72

## List of Figures and Tables

<b>Figure 1</b> – Structure of compact and cancellous bone.....	11
<b>Figure 2</b> – Types of cells found in bone.....	12
<b>Figure 3</b> – Example of medical conditions that require the application of bone grafts to surgically repair damaged tissue.....	14
<b>Figure 4</b> – Autografting procedure to repair collapsed disc.....	15
<b>Figure 5</b> – Scaffold-guided tissue regeneration.....	16
<b>Figure 6</b> – Simple culture techniques can not be used to grow organized tissue.....	16
<b>Figure 7</b> – Process diagram of the complete system.....	34
<b>Figure 8</b> – System assembled to produce HA.....	36
<b>Figure 9</b> – Etatron diaphragm metering pump and controller AG.....	37
<b>Figure 10</b> – Diffuser to add H <sub>3</sub> PO <sub>4</sub> .....	42
<b>Figure 11</b> – pH evolution without adding ammonia.....	47
<b>Figure 12</b> – XRD pattern of the experiments EN1 and EN2.....	48
<b>Figure 13</b> – XRD pattern of the experiments EN3 and EN4.....	49
<b>Figure 14</b> – XRD pattern of the experiments EN5 and EN6.....	50
<b>Figure 15</b> – XRD pattern of the experiments EN7 and EN8.....	50
<b>Figure 16</b> – XRD pattern of the experiments EN9 and EN10.....	51
<b>Figure 17</b> – XRD pattern of the experiment EN11.....	51
<b>Figure 18</b> – FTIR results of EN1.....	53
<b>Figure 19</b> – FTIR spectrum of EN2.....	53
<b>Figure 20</b> – FTIR spectrum of EN3.....	54
<b>Figure 21</b> – FTIR spectrum of EN5.....	54
<b>Figure 22</b> – FTIR spectrum of EN7.....	55
<b>Figure 23</b> – FTIR spectrum of EN8.....	55
<b>Figure 24</b> – FTIR spectrum of EN10.....	56
<b>Figure 25</b> – FTIR spectrum of EN11.....	56
<b>Figure 26</b> – Eh - pH diagram of the Ca-P-H <sub>2</sub> O system at 25°C for 1.67 molal activity of Ca and $a_{Ca}=1.67a_p$ .....	64

## List of Tables

<b>Table 1</b> – Standards for HA use in medicine according to ISO.....	34
<b>Table 2</b> – Experimental conditions used on experiment EN0.....	41
<b>Table 3</b> – Reagent quantities used to prepare the different batches of HA.....	42
<b>Table 4</b> – Reaction parameters used for the different samples.....	43
<b>Table 5</b> – HA purity based on XRD analysis.....	52
<b>Table 6</b> – Ca/P ratio and metals concentration of the experiments EN9 and EN10.....	56
<b>Table 7</b> – Phase composition of each sample based on XRD analysis.....	57
<b>Table 8</b> – Ca/P ratio based on quantity analysis (XRF).....	58
<b>Table 9</b> – Presence of elements on samples based on quality analysis (XRF).....	58
<b>Table 10</b> – Quantity of heavy metals measured for each sample.....	59

## **CHAPTER 1**

### **GENERAL INTRODUCTION**

## CHAPTER 1

### General Introduction

#### 1 - Overview

The preparation of hydroxyapatite (HA),  $[\text{Ca}_{10}(\text{PO}_4)_6(\text{OH})_2]$ , with specific characteristics regarding the grain morphology, stoichiometry, crystallinity and crystal size is important on biomedicine and materials science in order to meet a number of conflicting requirements for mechanical support and enhanced bone regeneration [1].

Biological apatites are nonstoichiometric and present nanometric crystal sizes in bone and dentin and micrometric in enamel. Synthetic HA can be used in many applications such as bioceramics and polymer composites for orthopaedic and dental applications in order to replace or augment small segments of bone. Its non medical applications include packing media for chromatography, gas sensors, catalysts and host materials for lasers [2].

In the past few years various methods for the preparation of HA crystals in the nanometric and submicrometric or micrometric size range have been developed [3]. The chemical composition of HA can be expressed by the ratio between calcium (Ca) and phosphorous (P). The theoretical value of Ca/P in HA is 1.67 [3]. Some methods produce nonstoichiometric Ca-deficient HA particles (Ca-dHA,  $\text{Ca/P} < 1.67$ ) and incorporate carbonate ions in the crystal lattice. In certain cases, the preparation of dense HA ceramics, stoichiometric rather than Ca-dHA is desirable. The reason is that segregation of  $\alpha$ - or  $\beta$ -tricalcium phosphate [ $\alpha$ - or  $\beta$ - $\text{Ca}_3(\text{PO}_4)_2$ ,  $\alpha$ - or  $\beta$ -TCP] occurs during sintering, which increases slow crack growth susceptibility and biodegradability of the HA ceramic [4]. Both characteristics are important for biomedical applications, once the selection of a material is a compromise between biocompatibility and mechanical performance [1, 2, 5].

Due to the increase demand of calcium phosphate materials, especially for biomedical applications, there is the need to develop a more continuous and reliable method for the preparation of HA with reproducible chemical and morphological properties.

## 2 - The Bone

Bone is a highly specialized form of connective tissue in which the extracellular matrix is mineralized, conferring marked rigidity and strength to the skeleton while still maintaining some degree of elasticity [6]. In addition to its supportive and protective functions, bone actively participates in maintaining calcium homeostasis in the body [6].

Bone is composed by two phases, an organic phase and mineral phase. The organic phase is mainly composed by collagen type I, approximately 95%, and the remaining 5% is composed of proteoglycans and numerous noncollagenous proteins [6, 7]; while the mineral phase is composed by calcium phosphate salts with a similar composition to HA.

Morphologically there are two forms of bone: cortical (compact) and cancellous (spongy). In cortical bone, densely packed collagen fibrils in adjacent lamellae run in perpendicular planes in plywood and cancellous bone presents a porous structure. The differences between cortical and cancellous bone are both structural and functional. Differences in the structural arrangements of the two bone types are related to their primary functions: cortical bone has a mechanical and protective function and cancellous bone is related to metabolic functions [6, 7].

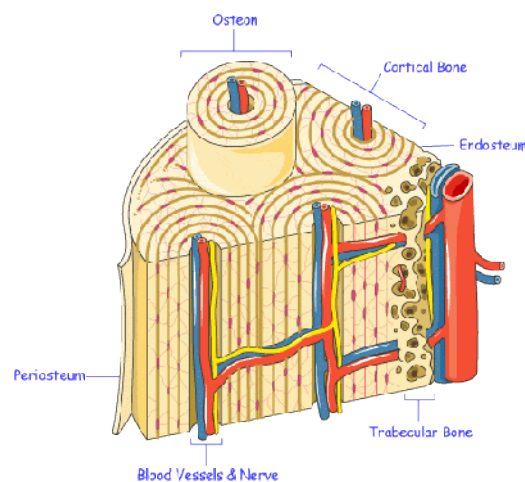


**Figure 1** - Structure of compact and cancellous bone [8].

There are five different cell types involved in bone formation and remodelling: osteoprogenitor cells, osteoblasts, osteocytes, osteoclasts, and lining cells [9].

Osteoprogenitor or osteogenic cells are mesenchymal cells that differentiate into osteoblasts. Their function is to respond to different metabolic demands or traumas, such as fractures, by differentiating into bone-forming cells, the osteoblasts [10]. So, osteoblasts are fully differentiated cells responsible for bone matrix formation and mineralization [11].

Osteocytes derive from osteoblasts which were trapped into the extracellular matrix. They are responsible for the maintenance of bone matrix and the rapid release of calcium and phosphorous from mineralized bone into the blood stream [9, 11].

Osteoclasts are multinucleated cells, originated from hematopoietic tissue and their function is bone resorption. Usually, they are located upon bone surfaces which are undergoing resorption [11-13].

Bone lining cells are present on bone surfaces where bone formation or resorption is not occurring [11]. Their function is to cover and protect bone surface and are thought to regulate the movement of calcium and phosphate in and out of the bone [10].

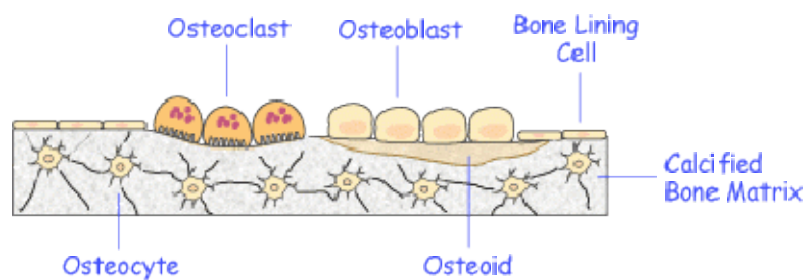


**Figure 2** - Types of cells found in bone [8].

During life, bone suffers a controlled process of remodelling that involves the resorption of older bone and the formation of new bone. The main function of this process is to enable bone to adjust to mechanical and metabolic demands placed upon the body [14].

Bone remodelling replaces fatigued or damaged bone, but when the bone loss exceeds new bone formation, the overall bone mass decreases and the risk of fracture raises. Numerous factors can contribute to this phenomenon, such as the constant use of drugs, age, hormones, degree of mobility, and genetics [15].

Currently, several therapies are available in order to preserve the equilibrium between bone formation and resorption, being most of them developed in order to

reduce bone resorption. However, when a substantial amount of bone has already been lost, reduction of bone resorption may not be sufficient to reduce the risk of fracture [16].

The development of biomaterials for bone regeneration is extremely important to increase the life quality and decrease the recovery period of patients who suffered from fractures and/or bone diseases. The biomaterials field has increased significantly in the last 20 years. A number of different materials such as metals, ceramics, polymers and composites are now commonly used to replace human bone [11, 13, 16].

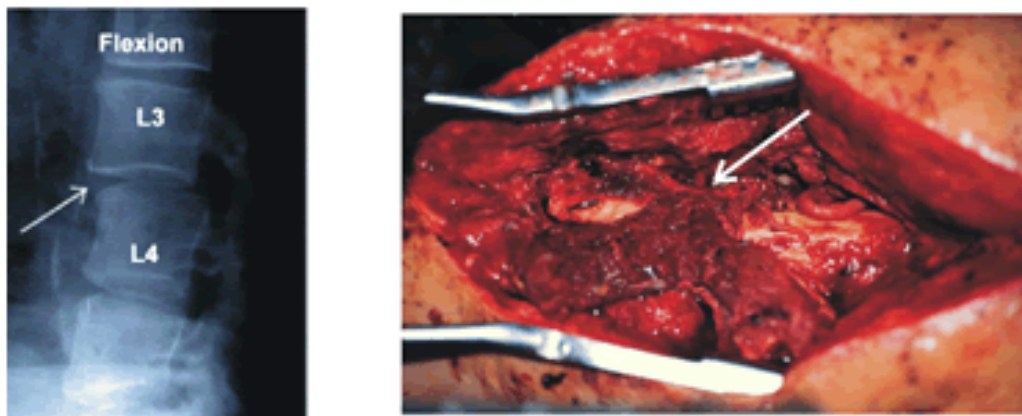
### **3 - Bone Graft Substitutes**

Bone grafts can be used to provide support, fill voids, and enhance repair of skeletal defects. They are used in several medical applications, such as: maxillofacial reconstruction, orthopaedics and dentistry [17].

The importance of bone graft and healing therapies is emphasized by the following:

*“The World Health Authority has decreed that 2000–2010 will be the Bone and Joint Decade, and this is now being supported by the United Nations. The rationale for this is that joint diseases account for half of all chronic conditions in people over 65; back pain is the second leading cause of sick leave; and osteoporotic fractures have doubled in the last decade, so that 40% of all women over 50 will eventually suffer from one. It is estimated that 25% of health expenditure in developing countries will be spent on trauma-related care by the end of the decade, and many children are deprived of normal development by crippling diseases and deformities.” [18]*

Many of the cases mentioned in the previous article will require the use of bone grafts to repair injuries or bone defects. Currently, there are over 500,000 bone grafts performed annually in the U.S. [19]. For example, it was estimated that 220,000 spinal fusions were performed in 1998, which required the use of bone grafts to secure areas of the spine affected by deformity, trauma, tumours, or degenerative disc disease (Figure 3a). There are approximately 170,000 fractures in the United States that fail to heal each year and also several fractures that have failed to heal within nine months (Figure 3b), which usually require the use of a bone graft to repair the fracture [19].



a. Collapsed disc.

b. Non-Union

**Figure 3** - Example of medical conditions that require the application of bone grafts to surgically repair damaged tissue [19].

A successful fusion remains dependent upon bone healing as well as the use of some form of bone graft.

An ideal bone graft should be osteogenic, have capacity to form bone and to carry living bone cells (osteoblasts, osteoclasts or their precursors); osteoinductive, its surface should stimulate osteoprogenitor cells to differentiate into bone forming cells in an osseous or non-osseous site; and osteoconductive, provide a bioactive surface where the osseous tissue can regenerate [20].

There are different types of bone grafts, which can be classified according to its origin:

- **Autografts** which involve harvesting bone tissue from the patient itself and transplanting it into a different area. When it is possible, the use of autologous grafts should be used because it has the best clinical outcomes. One of the most commonly performed autografts procedures is in spinal fusion surgery, where bone tissue from the patient's hip is harvested and implanted between the disc spaces of the spinal vertebrae or along the back of the spine (Figure 4). The grafted bone fuses the vertebrae together after several months [19]. Autografts are osteogenic, osteoinductive, osteoconductive, histocompatible and they do not represent a risk of disease transmission [20].

Autografting, however, has associated problems, such as: the morbidity at the harvest site can be significant causing problems such as pain, infection and blood loss.

Additionally, the surgical cost for the harvesting procedure is also a disadvantage [17, 21, 22].

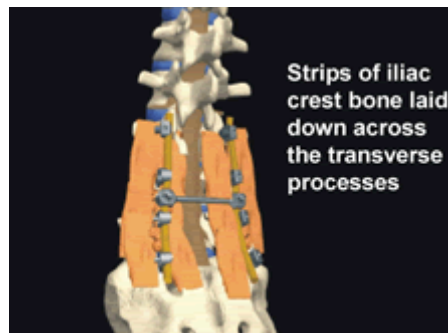


**Figure 4** - Autografting procedure to repair collapsed disc [19].

- **Allografts** involve harvesting and processing bone from a patient and transplanting it into another. Allografts are less successful than autografts due to immunogenicity reactions, the absence of viable cells and the risk of disease transmission [17, 19, 21].

- **Xenografts** consist in the transplantation of living cells, tissues or organs from one species to another, such as, pigs to humans and may represent a potential alternative to allografting when there are no human organs for transplantation.

Even though pig organs prove to function less well as human organs, they may be useful for short-term transplantation in patients waiting for an appropriate human organ [23-25].

- **Synthetic materials** include metals, polymers, and ceramics. These materials, however, are subject to fatigue, fracture, toxicity and do not adapt to the patient with time. A synthetic bone graft cannot grow with the patient and it cannot change shape in order respond to the loads placed upon the implant. For all these reasons, there is a real need for alternative bone substitutes and better wound healing therapies. Bone tissue engineering seeks to address this need [19, 21].

#### **4 - Bone Tissue Engineering**

Bone tissue engineering is a multidisciplinary and interdisciplinary field that applies the principles of biology and engineering to develop bone tissue substitutes to

restore, maintain, or improve the function of diseased or damaged human tissues. This form of therapy differs from standard drug therapy or permanent implants in that the engineered bone graft becomes integrated within the patient, stimulating the bone growth and being reabsorbed by physical, chemical or biological mechanisms [26, 27].

There are many approaches to bone tissue engineering, but all involve one or more of the following key properties: harvested cells, recombinant signalling molecules, and three-dimensional (3D) matrices. One approach, illustrated in figure 5, involves seeding highly porous biodegradable matrices (or scaffolds), in the shape of the desired bone, with cells and signalling molecules (protein growth factors) and then implanting the scaffolds into the defect to induce and guide the growth of new bone. The goal is for the cells to attach to the scaffold, multiply, differentiate and organize into normal, healthy bone as the scaffold degrades. The signalling molecules can be adhered to the scaffold or incorporated directly into the scaffold material [26, 27, 28].

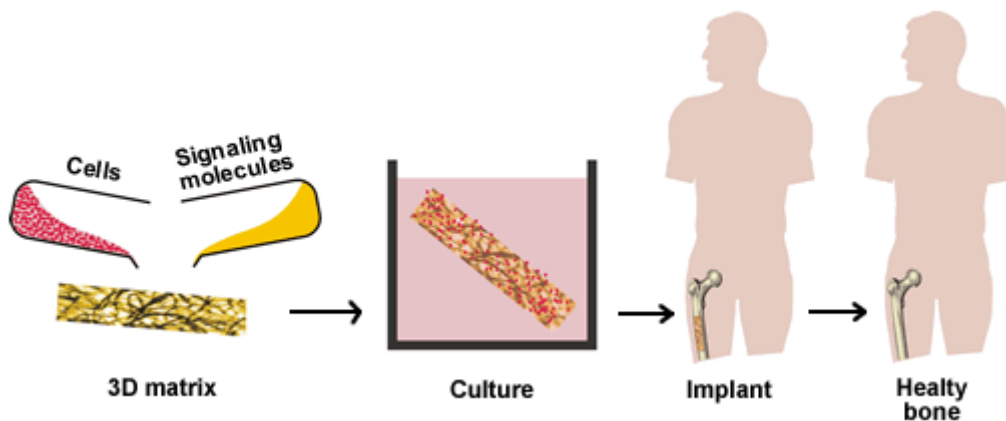


**Figure 5** - Scaffold-guided tissue regeneration [26].

It is not possible just to harvest some cells, such as osteoblasts, and then culture them to create a whole bone as depicted behind:

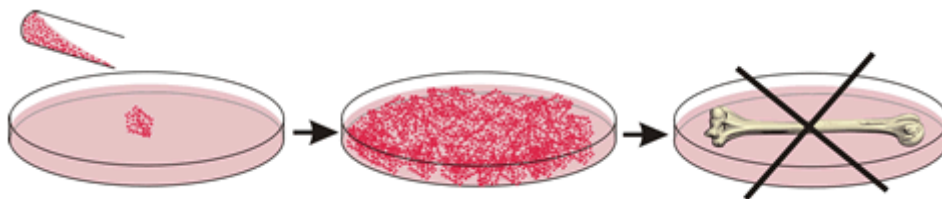


**Figure 6** - Simple culture techniques can not be used to grow organized tissue [26].

Conventional cell culture techniques involve growing cells in an artificial environment where they can thrive and replicate to form larger colonies of cells for applications such as in diagnostic tests. These colonies, however, do not become organized into tissues or organs that could then be implanted back into the patient. Cell colonies need external cues or signals to grow into functional 3D tissues or organs. In the body, cells are constantly stimulated with mechanical, electrical, structural, and chemical cues that guide the cells to their function. If these signals are not properly received or processed due to disease or trauma, then the cells become disorganized, and eventually die. The structural signalling involves the interaction of cells with their extracellular matrix (ECM). The ECM is that part of the human body which gives it form and shape [26, 27].

Tissue engineering techniques, such as shown in Figure 5, involve mimicking the natural environment by placing the cells and growth factors in synthetic scaffolds that act as temporary ECMs [26].

Another approach will be “*ex vivo* gene therapy” consisting on isolation of relevant stem cells or committed progenitors from mature adults or from animals, expand them *ex vivo*, transfect and select them *ex vivo*, and then reintroduce them *in vivo*. Genetic engineering, however, has numerous hurdles to overcome to make this approach reliable, practical, safe, and generally accepted [9, 27, 28].

The field of tissue engineering to repair or regenerate the musculoskeletal system is developing rapidly and expanding its applications. An American research group is trying to create tissue engineered bone using an advanced computer-aided-design/computer-aided-manufacturing (CAD/CAM) bioreactor system capable of growing large-scale, customized bone substitutes. A CAD model of the desired bone substitute would first be derived from the patient data [27]. The synthetic bone would then be prepared, in an advanced CAM bioreactor by depositing layers of biodegradable scaffolding material while simultaneously embedding it with the donor cells and growth factors within the layers. Synthetic vasculature would also be embedded within the scaffold as it is being built up. The scaffold structure, cellular distributions, and growth factor concentrations would be spatially varied using selective deposition. Additional osteogenic cues, such as mechanical stimulus, would be provided until the tissue was mature enough to be removed from the bioreactor and implanted into the patient. Such a system would also have applicability to other tissues and whole organs [27].

## 5 - Biomaterials

Since its beginning, just over a half century ago, the field of biomaterials has grown consistently with a steady introduction of new ideas and productive branches. A biomaterial can be defined as *a material intended to interface with biological systems to evaluate, treat, augment, or replace any tissue, organ, or function of the body* [29].

Biomaterials can be made of metals, polymers, ceramics, glasses, carbons, and composites materials [30].

Synthetic polymers, both organic and inorganic, are used in a wide variety of biomedical applications such as prosthetic implants, suture material and drug carriers [31] they can be biodegradable or nondegradable. Examples of biodegradable polymers are polylactic acid and polyglycolic acid, and copolymers. These polymers are currently used as suture materials, but are also being studied as bone, skin and liver substitutes [31]. Other biodegradable polymers currently under study for tissue engineering applications include polycaprolactone, polyanhydrides, and polyphosphazenes. Polymethylmethacrylate (PMMA), polytetrafluoroethylene (PTFE), and PMMA/polyhydroxyethylmethacrylate (PHEMA) which can be described as alloplastic and nonbiodegradable polymers. PMMA has considerable versatility and can be used for dentures, arthroplasties, cranioplasties, and as cement for many orthopaedic prostheses. PTFE has been used for augmentation and “guided bone regeneration” [32].

The principle of “guided bone regeneration” is that new bone formation will occur due to a “passageway” for progenitor cells and osteoblasts. To prevent soft tissue prolepsis into an osseous defect, a polymer membrane can be placed over a bone defect working as a reinforcement to guide bone, thereby deterring scar formation [32]. Physiologically, fibroblasts are more likely to populate an intraosseous defect than osteoblasts. Therefore, by sustaining a zone for migration of progenitor cells, the clinical outcome should be bone and not connective tissue scar [30, 32, 33].

Ceramics are also widely used in dental applications, and are being examined for bone tissue engineering applications. Two common ceramics used in dentistry and hip prostheses are alumina ( $\text{Al}_2\text{O}_3$ ) and HA. Alumina has excellent corrosion resistance, biocompatibility, high strength, and high wear resistance, and has been used for over 20 years in orthopaedic surgery [30, 32, 34].

HA is a calcium phosphate ceramic that has been used for over 20 years in medicine and dentistry. According to the literature HA is biocompatible, although its

biodegradation rate is very slow (a timeline of several years) [31, 32]. The degradation of HA can be controlled by varying its chemical composition such as the presence of tricalcium phosphate (TCP) that has a degradation rate faster than HA [1, 32].

The calcium sulphate known as Osteoset<sup>®</sup> (Wright Medical Corporation) is produced for orthopaedic application in non-stress bearing sites, such as the tibia plateau. Additionally, the aspirin-sized tablet of Osteoset<sup>®</sup> may find its use in the craniofacial skeleton to fill bone voids [35]. A combination product of calcium sulphate and tricalcium phosphate (Hapset<sup>®</sup>) has been suggested for dental applications, however, dental extraction sites heal uneventfully and the inclusion of foreign material is questionable [32].

Bioactive glasses can be used to repair damaged tissues, particularly hard tissues. The major advantage of these bioglasses is their ability to form a bond with the host tissue in a short period of time and the possibility to alter their chemical composition conferring them very specific which will allow their use in different clinical applications [32, 36, 37].

Bioactive glasses can be prepared by conventional technologies of the glass industry, but if the material is intended to be used in the medical field it is mandatory to analyse the purity of the raw materials to avoid any contamination. The different steps in the preparation of the material will influence its final characteristics. The Bioglass<sup>®</sup> 45S5 is the most studied glass and it is composed by 45 % in weight of SiO<sub>2</sub> and has a calcium/phosphorous molar ratio of 5:1. Glasses with significantly lower calcium phosphorous molar ratio do not form a bond with the bone and can not be used to prepare composites to apply in medical field [36, 37].

Native polymers, or extracellular matrix proteins, are commonly studied as graft materials. Collagens, which comprise a majority of proteins in connective tissue such as skin, cartilage and tendons, are popular candidates for such circumstances, and various collagen-based products are currently under studied [38]. When bone is demineralised with hydrochloric acid, the most common method, the bone derivative is largely composed by type I collagen and a minimal percentage of cell debris (a mix of soluble signalling molecules that are resistant to acidic demineralization) and also residues of ECM components. The form of the demineralised bone (DBM) can be particles, blocks, or strips. According to the literature [38], some clinicians have tested and approved the use of DBM products, while others have abandoned the use of these grafts. The variables influencing the clinical outcome from DBM therapy include non-standardized

procurement and preparation techniques, donor age and gender, quality control and sterilization. Clinical reports regarding the use of DBM and autograft demonstrate that these grafts have better results when they are used together and that DBM can be used as an autograft expander. Due to the strength limitations of collagen-based products, its dimensions are limited to small size and must be complemented by skeletal fixation [32, 39].

The polysaccharide hyaluronic acid (Hy), a glycosaminoglycan found in synovial fluid and cartilage, appears to be a promising material for bone tissue engineering. According to the literature [32], Hy induces chondrogenesis and angiogenesis during remodelling and is being studied individually and in combination with a collagen matrix for bone repair. Chondroitin sulphate is another glycosaminoglycan found in cartilage with potential applications as a bone tissue-engineered scaffold [32].

Composites of ceramics and polymers are an area of interest due to the possibility to obtain bone substitutes with a mix of properties from each of the respective components. Collagraft<sup>®</sup> is a synthetic bone graft comprised of collagen and a mineral mixture of HA and TCP (tricalcium phosphate). The biphasic ceramic of HA and TCP serves as a scaffold for bone growth, while the collagen serves as an extracellular matrix for bone growth. Collagraft<sup>®</sup> implant and Collagraft<sup>®</sup> strips have been approved for use in traumatic osseous defects and acute long bone fractures [40].

Another commercially available biomaterial is Bio-Oss<sup>®</sup> that is a natural, osteoconductive bone substitute that promotes bone growth in periodontal and maxillofacial osseous defects. It is composed of a bovine mineral portion of bone providing the body with a matrix for bone cell migration and integration into the natural physiologic remodeling process. Clinical success has been proven through years of experience and it is extensively documented in published scientific literature [41].

Healos<sup>®</sup> is sponge-like material composed of HA-coated collagen fibers that can be used as an osteoconductive matrix. It is generally accepted that the combination of collagen and calcium-based ceramics provides a bone-like matrix that supports the adhesion, migration, growth, and differentiation of bone-forming cells [32].

Bonelike<sup>®</sup> is a composite of HA reinforced with a P<sub>2</sub>O<sub>5</sub> based glass in order to increase simultaneously the mechanical properties of HA and to introduce ions commonly found in the mineral phase of bone [42-45]. This composite is prepared by a

liquid phase sintering route showing higher bioactivity and dissolution rate when compared to single phase HA. The incorporation of the glass induces the decomposition of HA in its secondary phases,  $\alpha$ -TCP and  $\beta$ -TCP, in a percentage depending on the glass content, composition and sintering conditions. Part of the  $\beta$ -TCP transforms into  $\alpha$ -TCP at high temperatures which improves the mechanical properties of Bonelike<sup>®</sup> [42-45]. Therefore, this composite can be used in medical applications which require higher degree of dissolution and faster healing process [42-45].

## 6 - Hydroxyapatite

The term "apatite" generally refers to a group of phosphate minerals, typically HA, fluorapatite or chlorapatite, having the general chemical formula  $\text{Ca}_5(\text{PO}_4)_3\text{X}$ , where X is OH<sup>-</sup>, F<sup>-</sup>, or Cl<sup>-</sup>, respectively.

The term "hydroxyapatite" refers to a form of apatite with the chemical formula  $\text{Ca}_5(\text{PO}_4)_3(\text{OH})$ , but is more typically represented as  $\text{Ca}_{10}(\text{PO}_4)_6(\text{OH})_2$  to denote that the crystal unit cell comprises two molecules [46]. HA is the hydroxylated member of the complex apatite group and has a Ca/P ratio of 1.667 [3, 46].

Seventy percent of bone is composed by a mineral phase similar to HA, which includes calcium phosphate, calcium carbonate, calcium fluoride, calcium hydroxide and citrate [47].

Nowadays, the use of HA as a filler for synthetic composites meant for bone augmentation and restoration is very common and an increasing number of new HA-containing biocompatible materials are reported every year [48].

### 6.1 – HA properties

HA is a good candidate for medical applications in which osteointegration is required. HA can be prepared in dense and macroporous form, with pores reaching up to 500  $\mu\text{m}$ . The dense HA can have up to 5% of porosity with a pore size inferior to 1  $\mu\text{m}$  and a crystal size lower than 2000 Å [36, 49].

The network of phosphate groups ( $\text{PO}_4^{3-}$ ) forms a structural skeleton that confers stability to HA which allows the substitution of different ions into its lattice. The substitution of the ions  $\text{Ca}^{2+}$ ,  $\text{PO}_4^{3-}$  and  $\text{OH}^-$  by others, such as,  $\text{K}^+$ ,  $\text{Na}^+$ ,  $\text{Mg}^{2+}$ ,  $\text{CO}_3^{2-}$

and  $F^-$ , alters the physical-chemical properties. Morphology, solubility and the cell parameters vary without substantial alterations of the hexagonal symmetry. A phase pure HA is theoretically composed in mass percentage by 39.68% of Ca and 18.45% of P, with a Ca/P mass ratio of 2.151, meaning a Ca/P molar ratio of 1.667 [50]. There are commercially available HA with molar Ca/P ratio different from 1.667. If the Ca/P ratio is lower than 1.667, the formation of different calcium phosphate phases is favoured, such as tetra phosphate Ca (TTCP) or  $\beta$ -TCP. If the Ca/P ratio is higher than 1.67 there will be the formation of calcium oxide (CaO), after a thermal treatment [3, 36, 49, 50, 51].

Thermodynamic analysis of the system Ca-P-H<sub>2</sub>O based on the development of the Eh-pH diagram show that HA predominates in the higher pH range, while Ca<sub>3</sub>(PO<sub>4</sub>)<sub>2</sub> and Ca<sub>2</sub>P<sub>2</sub>O<sub>7</sub> have their predominate pH range successively in the more acid direction. The pH range between 9 and 12 represents a very good stability of HA while the formation of secondary phases can occur for values of pH below 9. When the pH values exceed 12, the same diagram indicates the formation of Ca(OH)<sub>2</sub> causing the appearance of CaO [88].

About the mechanical behaviour of HA, according to the literature [36, 49], increasing the porosity decreases the mechanical properties while an increase on the sintering temperature increases the density, the resistance to twist, bending and compression. The tenacity to break has a maximum between 1100 and 1150 °C, decreasing at higher temperatures. Besides the influence of the preparation of the starting powder, the properties mentioned previously are governed by grain dimensions. It is however important to emphasize that the mechanical properties are better than those of the cortical bone, of the enamel and of the dentine. The break tenacity and the flexional rigidity decrease however in humid environment, so that the HA does not adapt for load-bearing applications, although its excellent biocompatibility and osteoconductivity. The *in vitro* dissolution of HA depends on the pH and on the saturation degree of the solution, on the crystallinity and on its composition. In the case of HA, it is also important the presence of defects, the type and the quantity of the micro and macroporosity. It is notable that the ceramic HA incur generalized dissolution (on the surface and inside the crystal), while the natural apatite dissolved selectively, particularly inside the crystal [3, 36, 49, 50, 51].

## 6.2 - Applications

HA has been intensively studied in the last decade in order to produce a third generation of bone grafts and implants to replace the prevalent allograft and metallic supports. HA is being used in several forms like powders, granules, and sintered porous blocks and even as coatings over metallic implants [52].

Coatings of HA are often applied to metallic implants (most commonly titanium alloys and stainless steel) to alter the surface properties. In this manner the body is able to accept HA due to its biocompatibility while, without the coating, the body would react to a foreign material and elicit an exacerbated inflammatory response. To date, the only commercially accepted method for applying HA coatings to metallic implants is by plasma spraying [53].

When large sections of bone have to be removed, for instance in case of bone cancers, or when bone augmentation is required (maxillofacial reconstructions or dental applications), HA can be employed to fill the bone defects or voids. The bone filler will provide a scaffold and encourage the rapid filling of the void by naturally bone forming cells, which provides an alternative to other bone grafts. HA will also become part of the bone structure and will reduce the healing period compared to the situation where no bone filling is used [22, 52, 53, 54].

Granules and blocks of HA are derived from powder and are mainly used as space fillers, scaffolds and low load bearing implants in orthopaedics. Nanosized HA powder (size <100 nm) with a uniform size and morphology has many applications in different fields of medicine ranging from targeted drug delivery to designed load-bearing implants. The need for new methods to prepare HA is nowadays relevant by the requirements of bone grafts with properties not just limited to biocompatibility; but also to bioactivity and resorbability, such functionality of HA can however be achieved only by exerting a control over its morphological features during synthesis. In biomedical industries, the absence of effective micro-structural control in co-precipitation processes is the main limitation in preparing functional HA nano-particles at a commercial level. Synthesis of nanosized HA powders from natural sources, though attractive, can never be a solution for the increase demand of HA in so many clinical applications [52, 53].

### 6.3 - Rules for Biomedical Application of Synthetic Hydroxyapatite

No known surgical implant material has ever been shown to cause absolutely no adverse reactions in the human body. However, long-term clinical experience of the use of HA has shown that an acceptable level of biological response can be expected, if the material is used on appropriate applications [55].

International Organization for Standardization (ISO) recognized the importance to create a standard to rule the application of HA in medicine and his Technical Committee dedicated to biomaterials prepared the ISO 13779, “Implants for Surgery – Hydroxyapatite” [55].

The document specifies requirements for ceramic HA intended for use as surgical implants as well as ceramic HA coatings applied to metallic or non-metallic surgical implants [55, 56].

Ceramic HA is recognized as HA which has been sintered into a coherent crystalline mass by subjecting it to conditions at which the crystals in the powder fuse together. Sintering is the process for production of ceramics in which the application of heat causes a significant reduction of particle surface area and bulk volume to achieve densification and consequent increase in mechanical properties [55].

The minimum content of crystalline HA should not be less than 95%. The maximum level for each of the other crystalline phases ( $\alpha$ -tricalcium phosphate ( $\alpha$ -TCP),  $\beta$ -tricalcium phosphate ( $\beta$ -TCP), tetracalcium phosphate (TTCP) and calcium oxide (CaO)) should be less than 5%. The calcium to phosphorus ratio, Ca/P, should have a value of  $1.65 \leq \text{Ca/P} \leq 1.82$  for the atomic ratio [55].

The maximum allowable limit for metals having adverse biological reactions is a total of 50 mg/kg distributed to Arsenic (3 mg/kg), Cadmium (5 mg/kg), Mercury (5 mg/kg) and Lead (30 mg/kg) [55].

Ceramic HA coatings is HA which has been deposited onto the surface of a metallic or non-metallic substrate either by means of a thermal spray process which produces a ceramic-type coating, or by means of a solution based technique which may deposit HA directly or may require thermal or other treatment to convert it into a crystalline form [56].

The calcium to phosphorus ratio, Ca/P, should have a value in the range of 1.67 to 1.76 for the atomic ratio. The limits of crystalline HA content and specific trace elements for ceramic HA coatings are the same as for ceramic HA [56].

ISO 13779 also specifies the methods that should be used to analyse the chemical composition and to assess the crystallinity and phase composition of HA-based materials such as coatings and sintered products. The foreign phase and the crystallinity ratio have to be determined from X-ray diffraction (XRD) [57]. Fourier transform infrared (FTIR) spectroscopy can be used to identify chemicals that are either organic or inorganic [57]. To determine Ca/P ratio X-ray Fluorescence Spectroscopy (XRF) must be used and the amount of trace elements (As, Cd, Pb and Hg) must be determined using Atomic Absorption Spectroscopy (AAS) [57].

## **6.4 - Preparation Methods**

The literature shows a number of methodologies for the preparation of HA and related phases, ranging from super-saturation of boiling solutions to low-temperature sol-gel-based synthesis, including hydrothermal conversion of calcium carbonate-containing marine invertebrates [3, 4, 58].

### **6.4.1 - Dry Method**

The dry method is available to prepare crystalline HA by employing a solid state reaction. For example, when brushite and calcium carbonate are used as a starting material, the following reaction occurs:



HA synthesized by the dry method is very fine, and the crystallinity is very high. As the reaction have to occur at more than 900°C, the process becomes more complicated than the wet method that gives similar results with simple conditions [3].

### **6.4.2 - Hydrothermal Method**

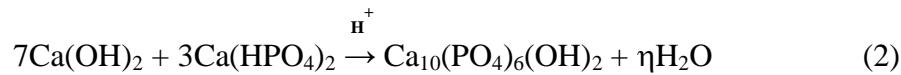
Hydrothermal synthesis has been used to transform slurries, solutions, or gels into the desired crystalline phase under mild reaction conditions typically below 350 °C. This method is appropriated to obtain large and perfect single crystals of HA. It is possible to prepare crystals of 10 nm using a reaction temperature of 300°C at a pressure

of 85 atm. The crystal lattice is better compared to other methods but the preparation time is between 24 and 72 hours and is frequent the presence of secondary phases [59].

Using this method with microwave power is possible to obtain crystals with diameters of 20-50 nm in small batches with a total reaction time of around 30 minutes. Hydrothermal method uses mixtures of  $\text{Ca}(\text{NO}_3)_2 \cdot 4\text{H}_2\text{O}$  with  $(\text{NH}_4)_2\text{HPO}_4$  or  $\text{H}_3\text{PO}_4$  with  $\text{Ca}(\text{OH})_2$  to prepare HA [60].

### 6.4.3 - Alkoxide Method

To prepare thin film HA the alkoxide method is available. The reaction occurs under temperatures between 500 and 1000°C and it is possible to use different starting materials [3], for instance according to the following chemical reaction [61]:



Along the years research was done using n-butanol or ethanol solutions of  $\text{P}_2\text{O}_5$  and calcium glycoxide as precursors of phosphor and calcium, but stable solutions of the precursors can be obtained in the presence of acetic acid (HOAC). For the solution of Ca glycoxide with the ethanol solution of  $\text{P}_2\text{O}_5$ , a lower HOAC/Ca ratio was needed since the ethanol solution of  $\text{P}_2\text{O}_5$  contained a lower concentration of  $\text{H}_3\text{PO}_4$ , a species that easily forms precipitates in the presence of the Ca containing species. The stable solutions of Ca glycoxide and the alcoholic solutions of  $\text{P}_2\text{O}_5$  were used to prepare HA coatings on alumina substrates using a dip-coating method. The resulting ceramic coatings have a rough surface and adhesion strength of about 10 MPa and the morphology presents a lot of limitations, concluding that this is not the best route to produce HA [62].

### 6.4.4 - Flux Method

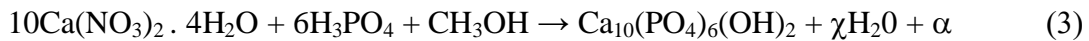
It is possible to prepare single crystals of HA by a flux method using  $\beta$ -tricalcium phosphate and  $\text{Ca}(\text{OH})_2$  under hot isostatic pressure [49].

HA whiskers were prepared by using the technique of molten salt synthesis with the fluxing agent of potassium sulphate ( $\text{K}_2\text{SO}_4$ ).

Flux Method is not appropriated to prepare phase pure HA but it is been used to prepare big single crystals of fluorapatite, chlorapatite, and boronapatite, using  $\text{CaF}_2$ ,  $\text{CaCl}_2$ , and  $\text{B}_2\text{O}_3$  flux. The reaction needs temperatures around  $1200^\circ\text{C}$  and can last up to 48 hours [3].

#### 6.4.5 – Sol-Gel Method

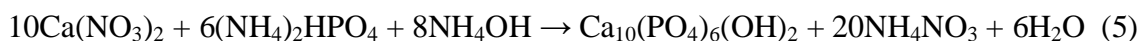
Recently, the use of sol-gel method for the synthesis of HA has become an important object of study. This process is a wet chemical method, which dispenses the use of high vacuum and high temperatures. It is considered one of the most flexible and promising techniques [63]. It is an elective method for preparing a highly pure powder because of the possibility of a careful control of the process parameters, favoured by a mixture at the molecular level of calcium and phosphorus ions that can improve the physical and chemical uniformity, resulting generally in a fine grain microstructure containing a mixture of submicron or nanosize crystals, which is very important to improve the reaction of contact and stability of the interface “artificial bone”/natural bone [64]. One example of the chemical reaction is the synthesis using phosphoric acid and calcium nitrate as calcium and phosphorous precursors, respectively. The solvent used is methanol [63]:



Although very promising, the HA prepared by this process presents crystallinity problems and the method is suitable only for the preparation of small quantities or thin layers of HA [63, 64, 65].

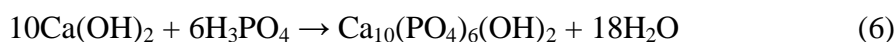
#### 6.4.6 - Wet Method

The wet method is utilized for mass production of small crystalline or non-crystalline powder. There are typically two kinds of process in the wet method. One involving the reaction of calcium salts and phosphate salts with the following chemical equation [66]:



The major disadvantage of this method is that the purity of the precipitated HA is affected by the purity of calcium nitrate. Furthermore, the excess of ammonia and ammonium by-products must be removed by extensive washing [3].

The other involves a neutral reaction of acid and alkaline solutions described by the following equation:



This method is the most convenient process and suitable for the industrial production of HA since it can produce larger amounts with good reproducibility and the only by-product is water [58, 67].

## 7 – Chemical Reactors and Surrounding Systems

The individual processes used by chemical engineers are called unit operations and consist of chemical reactions, mass transfer, heat transfer and momentum transfer operations. Unit operations are grouped together in various configurations for the purpose of chemical synthesis or chemical separation. Some processes are a combination of synthesis and separation operations.

A synthesis system normally involves the reagents treatment and transport, the chemical reactor, the product purification and a set of equipments to control the most important system parameters.

The more important parameters are temperature and pH, because they have direct influence in the final properties of the product. The temperature can be controlled by controlling the environment temperature, if there are no significant changes in temperature during the reaction, or to hold the reactor contents at a desired temperature, heat may be added or removed by heating or cooling coils or external jackets.

The control of pH is carried out through its constant measurement and the addition of an acid or a base solution which does not affect the reaction, to compensate for changes in pH over the reaction.

The unit operations needed to synthesize HA by the wet method are: the water purification system, the reactor with an effective stirring and a filtration unit.

## 7.1 – Chemical Reactors

In chemical engineering, chemical reactors are vessels designed to contain chemical reactions. The design of a chemical reactor deals with multiple aspects to maximize net present value for the given reaction. Designers ensure that the reaction proceeds with the highest efficiency towards the desired output product, producing the highest yield of product while requiring the least amount of money to purchase and operate. Normal operating expenses include energy, raw material costs and labour. There are three ideal chemical reactor types: Continuous Stirred-Tank Reactor (CSTR), Plug Flow Reactor and Batch Reactor [68, 69, 70].

In a CSTR, one or more fluid reagents are introduced into a tank reactor equipped with an impeller while the reactor effluent is removed. Simply dividing the volume of the tank by the average volumetric flow rate through the tank gives the residence time, or the average amount of time a discrete quantity of reagent spends inside the tank. Using chemical kinetics, the expected reaction completion can be calculated [68, 69].

The behaviour of a CSTR is often approximated or modelled by that of a Continuous Ideally Stirred-Tank Reactor (CISTR). All calculations performed with CISTRs assume perfect mixing. If the residence time is 5-10 times the mixing time, this approximation is valid for engineering purposes. The CISTR model is often used to simplify engineering calculations and can be used to describe research reactors. In practice it can only be approached, in particular in industrial size reactors [68, 69].

In a Plug Flow Reactor (PFR), one or more fluid reagents are pumped through a pipe or tube. The chemical reaction proceeds as the reagents travel through the PFR. In this type of reactor, the changing reaction rate creates a gradient with respect to traversed distance. At the inlet to the PFR the rate is very high, but as the concentrations of the reagents decrease and the concentrations of the products increase the reaction rate slows.

A PFR typically has a higher efficiency than a CSTR of the same volume. That is, given the same space-time, a reaction will proceed to a higher percentage completion in a PFR than in a CSTR [68, 69].

The batch reactor is the generic term for a type of vessel widely used in the process industries. This type of reactors is used for a variety of process operations such as: solids dissolution, product stirring, chemical reactions, batch distillation,

crystallization, liquid/liquid extraction and polymerization. In some cases, they are not referred to as reactors but have a name which reflects the role they perform (such as crystallizer, or bio reactor). A typical batch reactor consists of a tank with a stirrer and integral heating/cooling system [68, 69].

Liquids and solids are usually charged via connections in the top cover of the reactor, vapours and gases also discharge through connections in the top and liquids are usually discharged out of the bottom [68].

The advantages of the batch reactor lie with its versatility. A single vessel can carry out a sequence of different operations without the need to break containment. This is particularly useful when processing danger compounds [69].

The usual stirrer arrangement is a centrally mounted driveshaft with an overhead drive unit and impeller blades are mounted on the shaft. A wide variety of blade designs are used and typically the blades cover about two thirds of the diameter of the reactor. When viscous products are handled, anchor shaped paddles are often used which have a close clearance between the blade and the vessel walls [68].

Most batch reactors also use baffles, which are stationary blades that break up flow caused by the rotating stirrer. They may be fixed to the vessel cover or mounted on the side walls [68].

Despite significant improvements in stirrer blade and baffle design, mixing in large batch reactors is ultimately constrained by the amount of energy that can be applied. Much higher mixing rates can be achieved by using small batch reactors with high speed agitators [68].

## **7.2 – Water Purification**

Water purification is the process of removing contaminants and microorganisms from a raw water source. The goal is to produce water for a specific purpose with a treatment profile designed to limit the inclusion of specific materials. Most water is purified for human consumption (drinking water). Water purification may also be designed for a variety of other purposes as meeting the requirements of medical, pharmacology, chemical and industrial applications. Methods include ultraviolet light, filtration, water softening, reverse osmosis, ultra-filtration, deionization and powdered activated carbon treatment [71].

Water purification may remove: particulate sand; suspended particles of organic material; parasites, *Giardia*; *Cryptosporidium*; bacteria; algae; viruses; fungi; minerals such as calcium, silica, and magnesium; and toxic metals like lead, copper, and chromium [71].

### **7.3 – Filtration**

Filtration is a technique used either to remove impurities from an organic solution or to isolate an organic solid. The two types of filtration commonly used are gravity filtration and vacuum or suction filtration [70].

Gravity filtration is the method of choice to remove solid impurities from a liquid. The "impurity" can be a drying agent or an undesired side product or leftover reactant. Gravity filtration can be used to collect solid product, although generally vacuum filtration is used for this purpose because it is faster [70].

Vacuum filtration is used primarily to collect a desired solid, for instance, the collection of crystals in a crystallization procedure. Vacuum filtration uses either a Buchner or a Hirsch funnel and is faster than gravity filtration because the solvent or solution and air are forced through the filter paper by the application of reduced pressure. The reduced pressure requires that they be carried out in special equipment: Buchner or Hirsch funnel, heavy-walled, side arm filtering flask, rubber adaptor or stopper to seal the funnel to the flask when under vacuum and a vacuum pump [70].

## **CHAPTER 2**

### **DESIGN AND PROJECT DESCRIPTION**

## CHAPTER 2

### Design and Project Description

#### 1 - Introduction

The aim of the present project was to develop a system to prepare HA using the wet precipitation method with calcium hydroxide and ortho-phosphoric acid as reagents. It was aimed to prepare up to 500g of HA with a time reaction of 5 hours, having a specific control on the process parameters: temperature, pH, rate of reagent addition, and stir speed.

The pilot installation was designed by the author with the cooperation of the supervisors and researchers from the laboratory, based on the literature related with the wet precipitation method to prepare HA.

To prepare 500g of precipitated HA 20 liters of reagents are required. A chemical reactor must have a security coefficient around 25% in volume but, to carry out experiments to prepare higher quantities of HA, it was decided to design a reactor of 36 liters, optimizing the diameter and agitation to prepare 500g. It was also required a storage vessel for  $H_3PO_4$  and for  $NH_3$  (32%) and both vessels were constructed with a volume of 16 liters.

Vessels and reactor were made of Polyethylene, to avoid contamination and to resist to the chemical attack. The reagents used in the experiments were a strong base ( $Ca(OH)_2$  with a pH of 14) and a strong acid ( $H_3PO_4$  with a pH of 1). The base is classified as a corrosive solid and the acid is classified as a corrosive liquid. They can react with metals, acrylic and other polymers excluding Teflon, Polyethylene and Polyamide. The choice for Polyethylene was based in the following reasons: is easier to mould, is cheaper and completely avoids contamination.

The final product should have the characteristics showed on table 1, according to the values established by the International Organization for Standardization (ISO) for HA use in medicine [55, 56, 57].

The analyses were performed in the certificated laboratory CTCV (Centro Tecnológico da Cerâmica e do Vidro). The process diagram and single units are described below.

**Table 1** – Standards for HA use in medicine according to ISO 13779 [55, 56, 57].

<b>Phase Composition</b>	$\geq 95\%$ HA $\leq 5\%$ Secondary Phases
<b>Ca/P Ratio</b>	1.65 – 1.82
<b>Arsenic (As)</b>	$\leq 3$ mg/kg
<b>Cadmium (Cd)</b>	$\leq 5$ mg/kg
<b>Mercury (Hg)</b>	$\leq 5$ mg/kg
<b>Lead (Pb)</b>	$\leq 30$ mg/kg

## 2 – Process Diagram

The process diagram shows the components of the complete system and the connections between them.

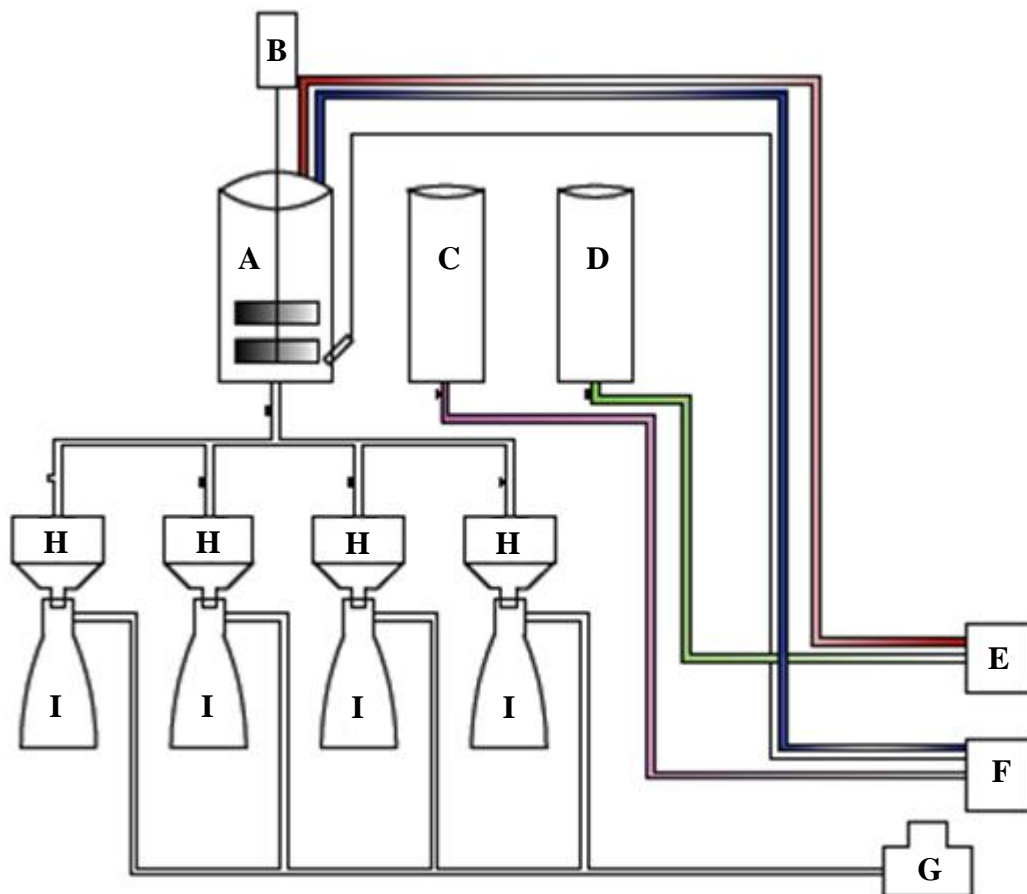


**Figure 7** - Process diagram of the complete system.

Legend:

A – Reactor;	D – H <sub>3</sub> PO <sub>4</sub> Vessel;	G – Vacuum Pump;
B – Stirrer;	E – H <sub>3</sub> PO <sub>4</sub> Pump;	H – Filtration Funnels;
C – Ammonia Vessel;	F – Ammonia Pump;	I – Filtration Tanks.

The HA preparation system was design to be easy to use and safe. In the beginning the bioreactor is filled with water and Ca(OH)<sub>2</sub> solution; the H<sub>3</sub>PO<sub>4</sub> solution is added with a calculated rate to the reactor from the vessel D forced by the pump E. The pH sensor inserted on the reactor is connected to the ammonia pump and monitors the pH inside the reactor. When the pH is less than 10.5, the pump F sends ammonia from the vessel C to the reactor, in order to increase the pH. After the reaction the pumps E and F are switched-off and the filtration is performed using the vacuum pump G; the HA stays in the filtration funnel H while the remaining liquid exits to the tanks I. After the reaction process, an after treatment of sintering at 1300 °C is required to achieve the quality and form of HA needed.

### **3 - Water Purification System**

The water purification system chosen was the *New Human Power III*, that is a system combining 2 functions, RO (Reverse Osmosis) and UP (Ultra Pure), producing pure water and ultra pure water simultaneously in a compact system. It can produce from the city/ground water, with a maximum of 35 l/h.

The comparison made with the other systems in the market proved that this system is more complete and reliable, with a capacity that feats the needs, including certification for medical applications.

The water obtained has a TOC of 0-5 ppb, less than 0.001 Eu/ml of endotoxins, less than 1 cfu/ml of bacteria and less than 1 µm/ml of particles. Pure water has 0.0-250.0 µs/cm while ultra pure water has 0.0 to 18.3 MΩxcm.

### **4 - Reaction System**

The bioreactor designed is composed by the reactor itself, the stir, the stir motor and a variable speed drive. The reactor has a volume of 36 liters with a diameter of 30

cm and a high of 50 cm. It allows a production from 100g to 600g of HA with a safety margin of 20% on the reactor volume.

The stir has a double shovel designed to maximize the agitation and prevent dead zones, with a variable speed drive Commander SE from Control Techniques.

The addition of  $H_3PO_4$  was carried out using an Etatron pump with adjustable flow rate up to a maximum of 5 l/h and is suitable to work with acids. Those were the main reasons to choose this pump.



**Figure 8** – System assembled to produce HA.

## **5 - pH Control System**

The pH control system is a junction of two equipments: diaphragm metering pump and a controller. The pump is a DLX from Etatron with acid-resistant plastic housing and the pump head is made of polypropylene, the diaphragm is PTFE and the seals are in Viton<sup>®</sup> (fluoroelastomer), to contact with corrosive solutions without any degradation effect. The characteristics of this pump and the possibility to have the same type of pump both for the acid addition and for the pH control were the main reasons having chosen it.

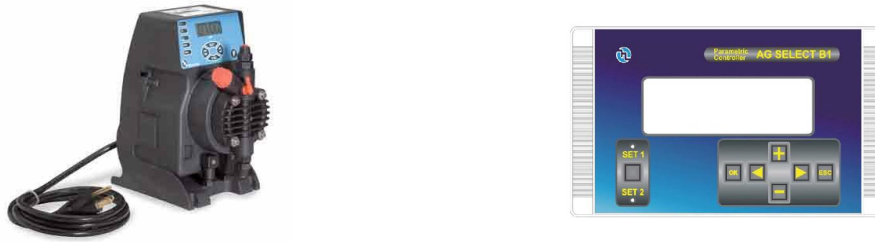


**Figure 9** – Etatron diaphragm metering pump and controller AG.

The controller is an AG Select B1 Parametric Controller, programmable for on/off or proportional control strategies. Control can be fine-tuned by programmable hysteresis and delay functions. Frequency of injections is programmable between 0 to 100% of the maximum flow rate of the pump (5 l/h).

## **6 - Filtration and Vacuum Systems**

The filtration system is composed by the filtration funnels, filtration vessels and a vacuum pump. Each funnel was design to have a volume of 5.5 l and each vessel has a volume of 10 l. With these capacities is possible to filter 20 l of product with a security margin of 10%. The vacuum pump is the ILMVAC MPC 201 E, a single-stage diaphragm pump consisting in pump housing and drive motor. It is a vacuum pump appropriated to dry and oil-free applications in the rough and medium-high vacuum range. The final vacuum is < 75 mbar, the suction rate is 1.8 m<sup>3</sup>/h and is chemical-resistant.

## **7 – Powder Preparation and Sintering**

To obtain fine powders under 75  $\mu\text{m}$ , HA was crushed and milled in a planetary mill Pulverisette 6 from Fritsch with agate ( $\text{SiO}_2$ ) grinding bowl and agate grinding balls to avoid contamination.

This equipment has a laboratory mill design with only one grinding bowl and operates according to the principle of the planetary ball mills. As principal features it has a very high grinding performance with low space requirements grinding samples down to < 1 $\mu\text{m}$  and reproducible grinding result thanks to regulated drive and programmable electronics. It has certified safety EN 61010 and CE mark.

The equipment used to sieve the product was a Retch Vibratory Sieve Shaker containing stainless steel sieves of 250, 120 and 75  $\mu\text{m}$ .

The sintering furnace is a bottom loading muffle furnace from Termolab with a Eurotherm controller and the advantage of having a system of loading and sealing. The elements of heating are installed in the four side walls permitting an excellent profile of temperature throughout the chamber. The sintering was made at 1300°C using a heating rate of 4°C/min with 1 hour residence time at 1300°C, followed by natural cooling inside the furnace.

## **CHAPTER 3**

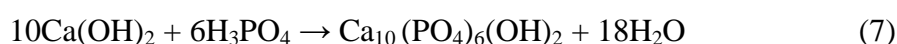
### **EXPERIMENTAL PROCEDURES**

## CHAPTER 3

### Experimental Procedures

#### 1 - Introduction

This chapter describes the laboratorial procedures for the preparation and physicochemical characterisation of HA. HA was prepared through a wet precipitation method that consists on the reaction between calcium hydroxide,  $\text{Ca}(\text{OH})_2$ , and ortho-phosphoric acid,  $\text{H}_3\text{PO}_4$ , as described by the following equation:



During the synthesis process, an aqueous solution containing  $\text{H}_3\text{PO}_4$  was added through a peristaltic pump to a suspension containing  $\text{Ca}(\text{OH})_2$  in distilled water, maintained with vigorous stirring.

The pH was monitored during the reaction time and was controlled by the addition of ammonia solution,  $\text{NH}_3$  (32%), keeping the pH values above 10.5.

The final solution was left ageing overnight and the resulting precipitate was filtrated through the vacuum system described before, using paper filters without ashes to avoid contamination. The resulting product was dried in an oven at  $60^\circ\text{C}$ , for two days.

Each sample was sintered in a muffle furnace at  $1300^\circ\text{C}$  using a heating rate of  $4^\circ\text{C}/\text{min}$  with 1 hour residence time at  $1300^\circ\text{C}$ , followed by natural cooling inside the furnace.

After sintering HA was crushed and milled in an agate planetary mill to avoid contaminations. Then was sieved under  $75\ \mu\text{m}$  (250, 120 and  $75\ \mu\text{m}$  stainless steel sieves), to destroy the agglomerates.

All the samples were then analysed using the X-ray Diffraction (XRD) and, depending on the result of XRD, some samples were selected to be analysed by Fourier Transform Infrared (FTIR), X-ray Fluorescence Spectroscopy (XRF) and Atomic Absorption Spectroscopy (AAS).

## 2 - Evaluation of pH Levels

In order to evaluate the pH variation during the reaction, the control experiment EN0 was carried out without the addition of ammonia. This test was important to determine the time when the pH reaches the value of 10.5 that is the equilibrium point when the addition of ammonia is needed. This addition will avoid the displacement of the reaction in the inverse way. The conditions used in EN0 are described in table 2.

**Table 2** – Experimental conditions used on experiment EN0.

<b>Sample</b>	<b>EN0</b>
HA (g)	200
Ca(OH) <sub>2</sub> (g)	148.19
H <sub>3</sub> PO <sub>4</sub> (g)	138.35
H <sub>2</sub> O (l)	8
32% NH <sub>3</sub> (ml)	0
H <sub>3</sub> PO <sub>4</sub> Addition Rate (ml/min)	31
Stir Speed (rpm)	70
Time (min)	130

This experiment allowed also the determination of the optimum stir speed that was optimized to maximize turbulence and minimize splashing.

## 3 - Experiments to achieve 500g of HA according to ISO 13779

After the control experiment, a set of experiments was carried out in order to evaluate the ability of this system to achieve the main objective of this work, the preparation of 500 g of HA using this new equipment.

The experiments started with the preparation of 100g of HA optimizing all the parameters. Each sample was analysed by XRD and FTIR; when the purity obtained for 100 g (EN1 and EN2) was according to ISO 13779 [55], was tried an increase of 100g of HA to be prepared (EN3 and EN4) and this procedure was repeated until the value of 500g (EN9 and EN10). Table 3 describes the amount of HA prepared and the correspondent reagent quantities needed for all the experiments.

The sample EN11 was prepared to investigate the ability of the system to produce 600g of HA per batch. Each experiment was repeated between 3 or 4 times and were selected 2 samples from each quantity of HA prepared.

**Table 3** – Reagent quantities used to prepare the different batches of HA.

<b>Sample</b>	<b>HA (g)</b>	<b>Ca(OH)<sub>2</sub> (g)</b>	<b>H<sub>3</sub>PO<sub>4</sub> (g)</b>	<b>H<sub>2</sub>O (l)</b>
<b>EN1</b>	100	74.10	69.17	4
<b>EN2</b>	100	74.10	69.17	4
<b>EN3</b>	200	148.20	138.35	8
<b>EN4</b>	200	148.20	138.35	8
<b>EN5</b>	300	222.29	207.52	12
<b>EN6</b>	300	222.29	207.52	12
<b>EN7</b>	400	296.38	276.69	16
<b>EN8</b>	400	296.38	276.69	16
<b>EN9</b>	500	370.48	345.87	20
<b>EN10</b>	500	370.48	345.87	20
<b>EN11</b>	600	444.57	415.04	24

Table 4 describes the reaction conditions of each sample along the experiment time, starting with small HA quantities and low addition rate of H<sub>3</sub>PO<sub>4</sub> until the preparation of large quantities and higher addition rate.

From sample EN9 to EN11 a diffuser developed during this work was used to add the H<sub>3</sub>PO<sub>4</sub> (Figure 10).



**Figure 10** - Diffuser to add H<sub>3</sub>PO<sub>4</sub>.

The diffuser was developed in order to prevent the splashing effect onto the reactor wall and also to create new reaction regions which should allow a faster addition rate of the  $H_3PO_4$  solution. The cover of the bioreactor was adapted to experiment different configurations of the diffuser and the use of four addition points was found to be the more efficient.

In this set of experiments the parameters tested were the quantity of HA prepared, the addition rate of  $H_3PO_4$  and the way as the ammonia was added. For the experiments EN1 to EN5 the automatic system to add ammonia was used revealing some problems so in the experiments after EN5 the addition of ammonia was always made manually and at once using the information studied in the experiment EN0.

The minimum pH achieved during the reaction was monitored throughout the experiments and the value is also presented in Table 4.

**Table 4** – Reaction parameters used for the different samples.

<b>Sample</b>	<b>HA (g)</b>	<b><math>H_3PO_4</math> Addition (ml/min)</b>	<b>Stir Speed (rpm)</b>	<b>Minimum pH</b>	<b><math>NH_3</math> (ml)</b>	<b>Time (min)</b>
<b>EN1</b>	100	8.3 ml/min	70 rpm	10.52	120	240
<b>EN2</b>	100	11.1 ml/min	70 rpm	10.50	60	180
<b>EN3</b>	200	11.1 ml/min	70 rpm	10.51	120	360
<b>EN4</b>	200	15.5 ml/min	70 rpm	10.57	120	260
<b>EN5</b>	300	15.5 ml/min	70 rpm	10.55	450	390
<b>EN6</b>	300	15.5 ml/min	70 rpm	10.53	200	390
<b>EN7</b>	400	15.5 ml/min	70 rpm	10.50	300	520
<b>EN8</b>	400	31 ml/min	70 rpm	10.60	300	260
<b>EN9</b>	500	31 ml/min	70 rpm	10.59	350	325
<b>EN10</b>	500	31 ml/min	70 rpm	10.57	350	325
<b>EN11</b>	600	31 ml/min	70 rpm	10.63	400	390

The experiment EN1 was performed using an addition rate of 8.3 ml/min while EN2 used 11.1 ml/min. EN3 maintained all the parameters of EN2 but the amount of HA prepared was the double and also the amount of ammonia added was the double. EN4 was performed with an adding ratio of 15.5 ml/min and the same conditions were maintained to the preparation of 300g of HA in EN5. The amount of ammonia added on

the experiment EN5 was 450 ml, which is a much higher amount in comparison to the 60 ml added on EN2 and the 120 ml added on EN3 and EN4.

The experiment EN5 was repeated using the same conditions (EN6) adding only 200 ml of ammonia at once and this amount was enough to maintain the pH above 10.5. The experiment EN7 used the same parameters of EN6 to prepare 400 g of HA instead of 300 g and in EN8 the adding ratio was 31.1 ml/min instead of 15.5 ml/min. The conditions were maintained in EN9 and EN10 that are the experiments corresponding to the main objective of this work: prepare 500 g of HA in 5 hours. The sample EN11 was prepared to evaluate the ability of the system to the preparation of 600 g of HA per batch.

After this set of experiments that allowed the preparation of 500g of HA, the conditions of samples EN9 and EN10 were applied in 23 experiments to verify the reproducibility of the bioreactor and to allow statistical analysis, which will confirm the ability of the system for the medical certification, to produce HA for medical applications. These conditions correspond to the preparation of 500g of HA per batch that was the value used to design the reactor.

#### **4 - Sample Characterisation**

The HA sintered powders of the experiments EN1 to EN11 were characterised using XRD analysis carried out in the laboratory of the University of Aveiro (Departamento de Cerâmica e Vidro da Universidade de Aveiro) and FTIR analysis carried out in the laboratory of Instituto Nacional de Engenharia Biomédica (INEB). XRD analyses were performed using a Rigaku Dmax-III-VC diffractometer, with a  $\text{Cu-K}\alpha$  radiation ( $K\alpha = 1.54056$  Angstroms) and the data was collected from 4 to 80° ( $2\theta$ ), with step size of 0.02°/s. The method used to quantify the phase formation was the calculation of the relative height of the main peaks correspondent to HA ( $2\theta = 31.773^\circ$ ),  $\alpha$ -TCP ( $2\theta = 30.751^\circ$ ),  $\beta$ -TCP ( $2\theta = 31.026^\circ$ ) and CaO ( $2\theta = 37.800^\circ$ ), and the results were compared to the limits described in ISO 13779 [55]. From the XRD results was calculated the percentage of each phase present in each sample. For the experiments EN0 to EN11, this calculation was performed comparing the main peak of HA with the main peak of the secondary phases.

FTIR analyses were performed using the equipment Perkin-Elmer 2000, with  $4\text{cm}^{-1}$  resolution and 100 scans. To analyse the samples, HA powders were mixed with potassium bromide (2mg HA / 200mg KBr) to form a thin disc using a steel die in a uniaxial press.

For the samples EN9 and EN10, which represent the final objective of this work, were performed more specific analyses in the laboratory CTCV (Centro Tecnológico da Cerâmica e do Vidro), that is a certified laboratory which would allow for the medical certification of the bioreactor to produce HA for medical applications. The analyses were performed in order to determine:

- Ca/P ratio using X-ray Fluorescence Spectroscopy (XRF);
- The concentration of heavy metals (As, Cd, Pb and Hg) using Atomic Absorption Spectroscopy (AAS).

The other set of 23 experiments carried out with conditions of EN9 and EN10, were also quality and quantity analysed in the certified laboratory of CTCV to determine the phase percentage of each sample using XRD, the Ca/P ratio using XRF, the presence of elements and the concentration of heavy metals using AAS.

The calculation of the phase content made by CTCV was based on the Matrix Flushing Model that compares the intensity obtained for each phase of the experimental samples with standard samples of compounds of known concentrations. The background correction of the measured intensities is also applied by this model.

According to ISO 13779 [55], the minimum content of crystalline HA is 95% and the maximum level of the other crystalline phases,  $\alpha$ -tricalcium phosphate ( $\alpha$ -TCP),  $\beta$ -tricalcium phosphate ( $\beta$ -TCP), tetracalcium phosphate (TTCP) and calcium oxide (CaO), should be less than 5%. The calcium to phosphorus ratio, Ca/P, should have a value between  $1.65 \leq \text{Ca/P} \leq 1.82$ . The maximum limit for heavy metals is 50 mg/kg distributed to Arsenic (3 mg/kg), Cadmium (5 mg/kg), Mercury (5 mg/kg) and Lead (30 mg/kg) [55].

The results obtained were used to calculate the average and standard deviation of the phase purity and Ca/P ratio in order to confirm the capabilities and reproducibility of the bioreactor.

## **RESULTS**

## RESULTS

### A - Evaluation of pH level

Orthophosphoric acid (0.3M) was added dropwise to a calcium phosphate solution (0.5M) for 130 minutes without the addition of ammonia, in order to assess the pH variation throughout the reaction time (EN0). The resulting titration curve allowed the determination of the equivalence point at 110 minutes, approximately 2/3 of the total reaction time (Figure 11), determined by the tangent method.

This test was important to assess the equivalence point, which would allow the determination of the time from which the addition of ammonia was needed. Until experiment EN5 the ammonia was automatically added, after which ammonia was added manually at approximately 2/3 of the reaction time, as determined by the titration curve.

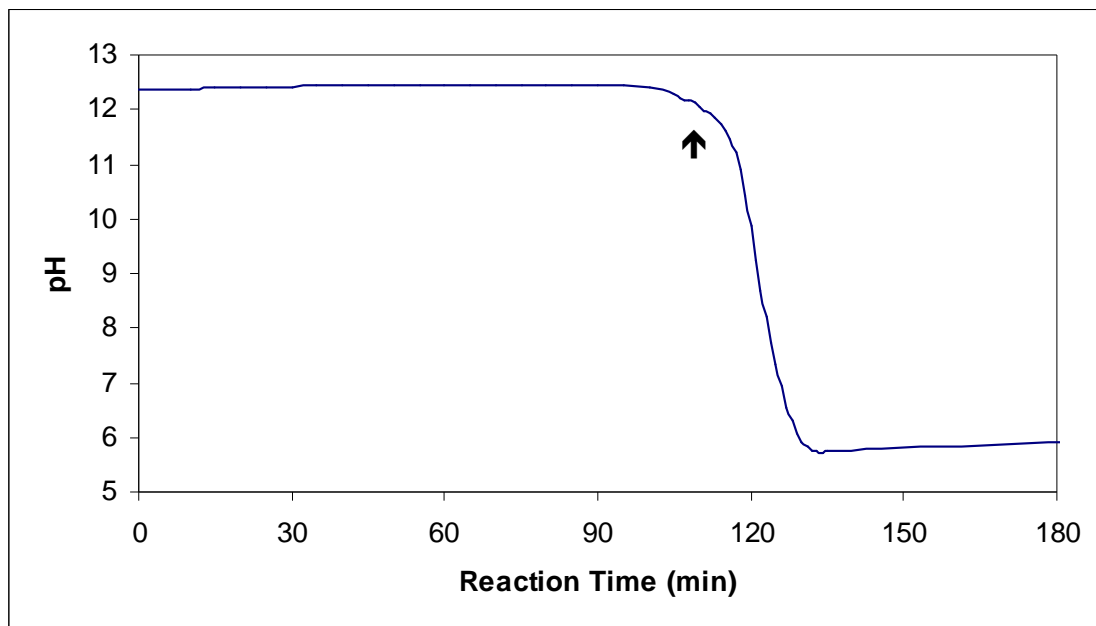


**Figure 11** – pH variation without the addition of ammonia.

The XRD analysis of the sample EN0 (data not shown) revealed the presence of three phases: HA (69%),  $\alpha$ -TCP (24%) and  $\beta$ -TCP (7%). This calculation was performed comparing the main peak of HA with the main peak of the secondary phases.

### B – Preparation of HA

In order to evaluate the effect of the addition rate of  $H_3PO_4$  several experiments were carried out, starting from 100g batches of HA (EN1 and EN2). XRD analyses were performed for all the samples and the HA phase purity (Table 6) was calculated based on XRD results, as described on the experimented procedures chapter.

EN1 was prepared using an addition rate of 8.3 ml/min of  $H_3PO_4$  and in order to maintain the pH above 10.5, 120 ml of  $NH_3$  was added, but when the acid addition rate was increased to 11.1 ml/min, the quantity of  $NH_3$  added was 60 ml (EN2). This may be due the increase of the acid addition rate or a problem in the automatic system.

Analysing the XRD pattern for the EN1 sample two phases were detected (HA and CaO), while for EN2 only the presence of HA was observed.

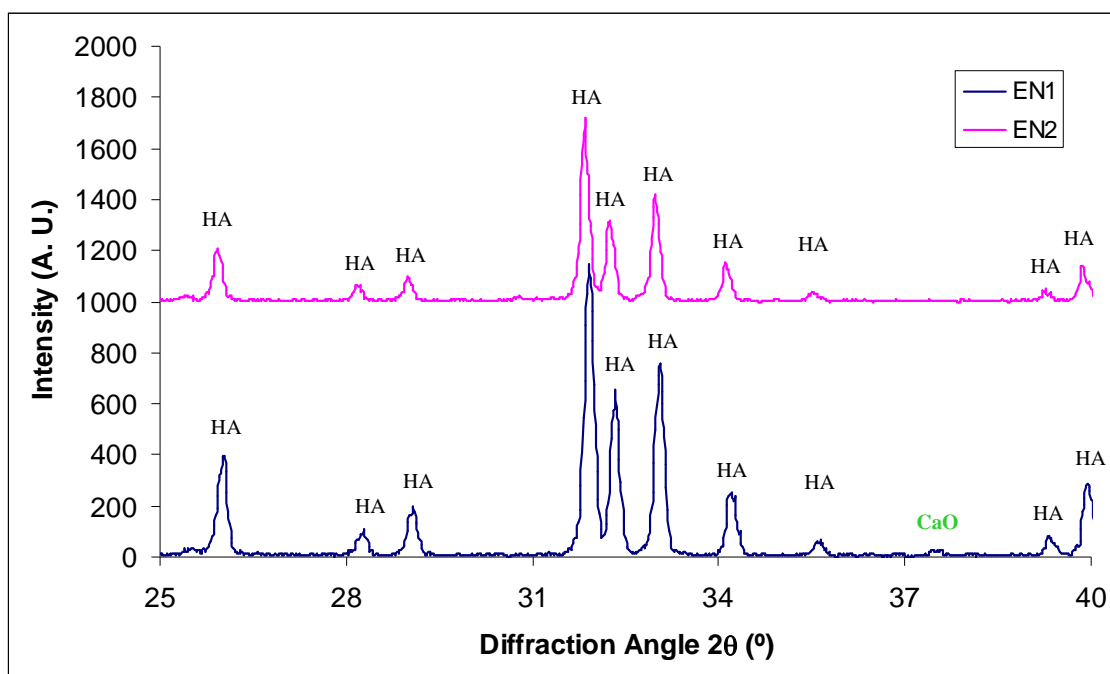


**Figure 12** – XRD pattern of the experiments EN1 and EN2.

As the XRD pattern of EN2 only presents the phase corresponding to HA, a new experiment was carried out using the same conditions, but in this case the amount of HA prepared was 200g (EN3). On EN3 XRD pattern, no secondary phases were detected; therefore, the addition rate of  $H_3PO_4$  for EN4 was increased to 15.5 ml/min in order to verify if it is possible to prepare the same quantity of HA spending less time. Again no secondary phases were detected on the XRD pattern. The quantity of ammonia needed to maintain the pH above 10.5 was 120 ml in both experiments revealing no interference of the acid addition rate on the quantity of ammonia added.

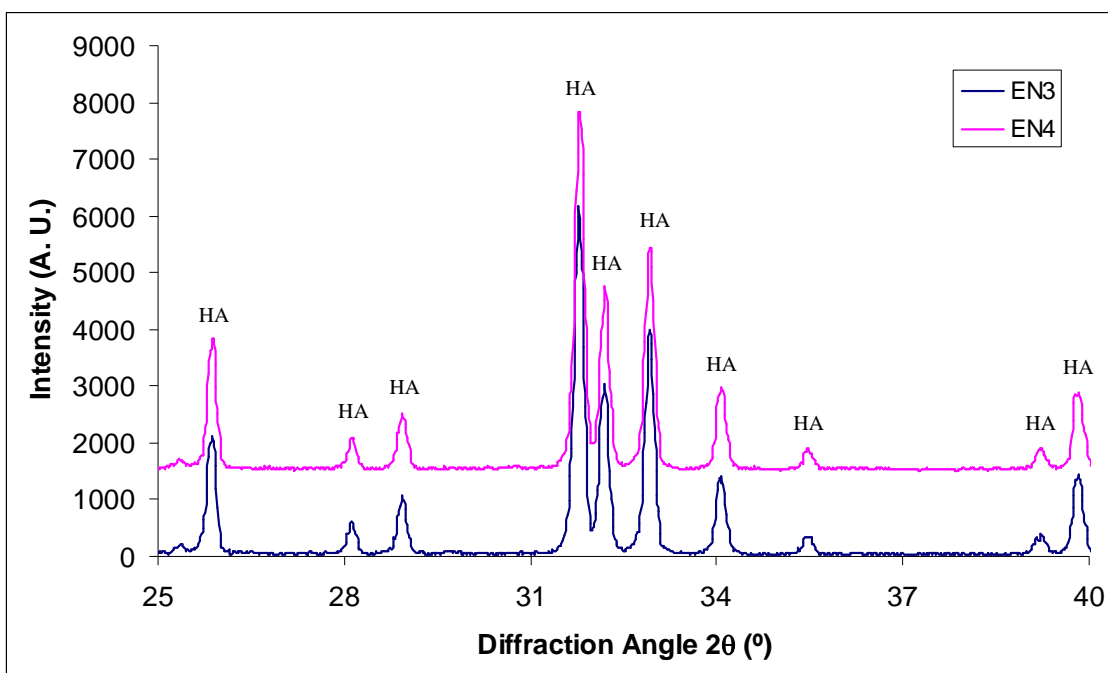


**Figure 13** – XRD pattern of the experiments EN3 and EN4.

The conditions used for EN4 were applied to prepare 300g of HA (EN5). The  $H_3PO_4$  addition rate was 15.5 ml/min and the quantity of ammonia added was 450 ml. EN5 XRD pattern demonstrates the presence of HA,  $\alpha$ -TCP and CaO. Due to the large amount of ammonia added, the conditions of this experiment were repeated in EN6, but the ammonia was added manually, to verify if it was a problem with the ammonia addition system and the ammonia needed was only 200 ml. The XRD pattern for EN6 presents just the phase corresponding to HA, therefore, it seems that a higher amount of ammonia may induce the formation of secondary phases. Due to the results obtain in EN5 and also in EN1, it was decided that ammonia would be added manually and at once, using the data obtained from experiment EN0 and also from the optimized relation between the quantities of HA prepared and the quantity of ammonia needed.

The same conditions of EN6 were used to prepare 400g of HA (EN7). The acid addition rate was again 15.5 ml/min for EN7 and the result obtained for the calculated purity was 98.5% (Table 6), so an increase to 31 ml/min was performed for EN8. The quantity of ammonia needed to maintain the pH above 10.5 was 300 ml in both experiments. The XRD pattern for experiments EN7 and EN8 are illustrated in Figure 15, where it is possible to observe the presence of the HA phase and the secondary phase CaO, for the EN7 while the EN8 pattern exhibits the presence of HA and the secondary phase  $\alpha$ -TCP.

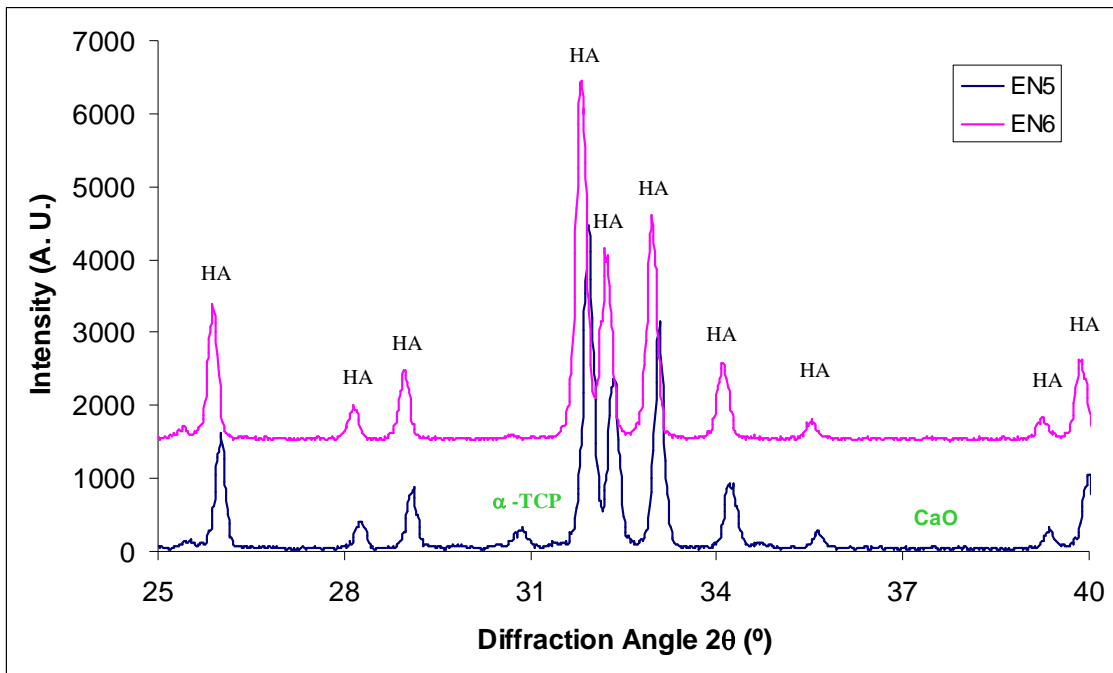


**Figure 14** – XRD pattern of the experiments EN5 and EN6.

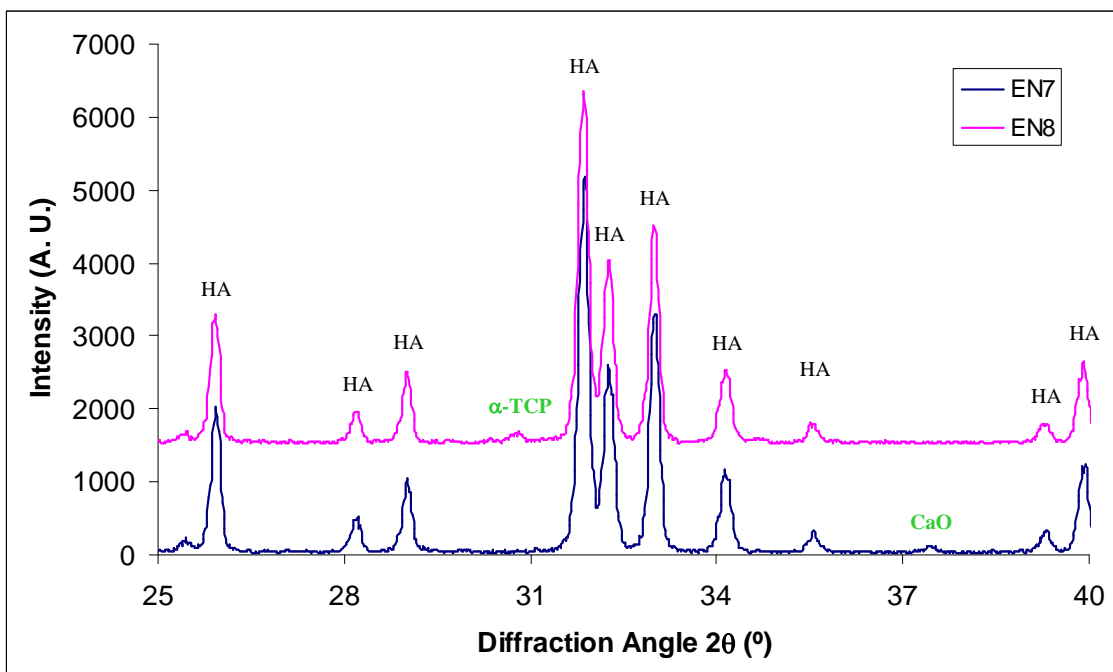


**Figure 15** – XRD pattern of the experiments EN7 and EN8.

Although, on the XRD pattern for EN8 there was the presence of secondary phases two new experiment were carry out, but in this case 500 g of HA were prepared using the diffuser system to add the acid solution. The  $H_3PO_4$  addition rate was 31 ml/min and the quantity of ammonia added manually to maintain the pH above 10.5 was

350 ml in both experiments. The XRD patterns for EN5 and EN10 experiments demonstrate that the 500g batches were phase pure HA (Figure 16).

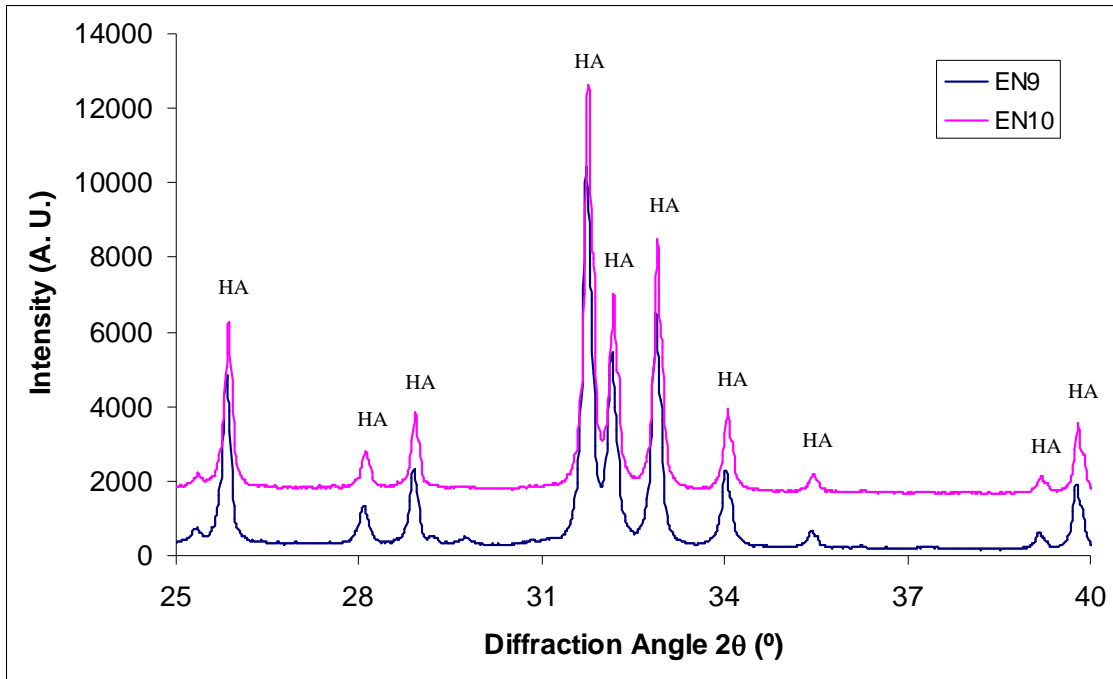


**Figure 16** – XRD pattern of the experiments EN9 and EN10.

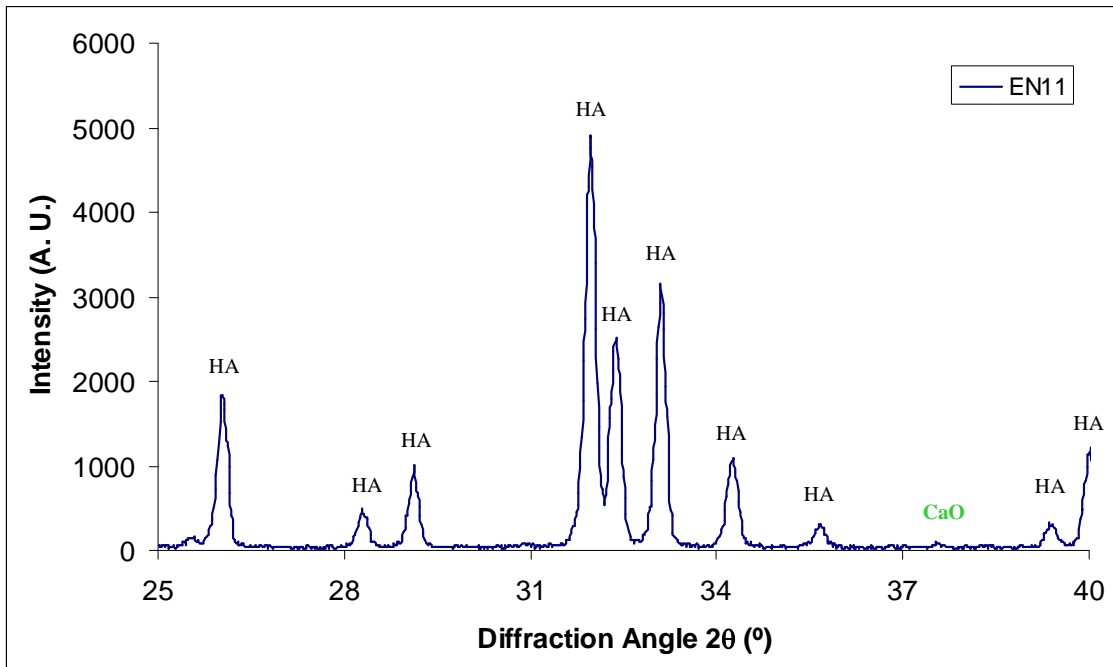


**Figure 17** – XRD pattern of the experiment EN11.

The conditions used on experiment EN9 and EN10 were used on the preparation of 600g of HA, again the  $H_3PO_4$  addition rate was 31 ml/min, but the quantity of

ammonia added was 400 ml. The XRD pattern (Figure 17) shows the presence of HA as well as a small percentage of CaO.

From the XRD analysis, the HA phase content of each sample was calculated. The determination was done based on the relative intensity of HA peaks and secondary phases  $\alpha$ -TCP,  $\beta$ -TCP and CaO, containing an error related to these calculations of  $\pm 1\%$ .

**Table 5** – HA purity based on XRD analysis.

Sample	EN1	EN2	EN3	EN4	EN5	EN6	EN7	EN8	EN9	EN10	EN11
<b>HA Prepared (g)</b>	100	100	200	200	300	300	400	400	500	500	600
<b>HA Phase (%)</b>	97.6	100	100	100	96.5	100	98.5	97.9	100	100	97.6

Even considering the error associated to these results, the HA phase present in all experiments is in accordance with the value fixed by ISO 13779 for the use of HA in medical applications, which is 95% [55].

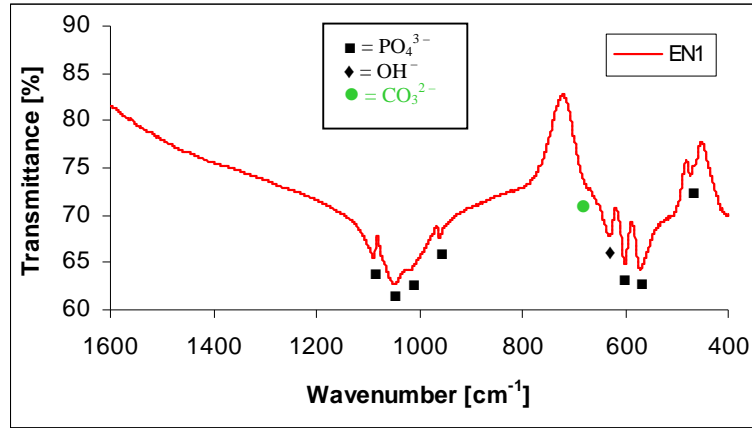
From the XRD pattern of EN2, EN3, EN4, EN6, EN9 and EN10 was not possible to identify secondary phases or contaminants, and the calculations confirmed that the samples are phase pure HA, as it is possible to verify in Table 5.

### **C - Evaluation of functional groups using FTIR analyses**

The FTIR spectra of all samples display the characteristic bands of HA, the hydroxyl ( $\text{OH}^-$ ) at  $630\text{ cm}^{-1}$  and phosphate groups ( $\text{PO}_4^{3-}$ ) at 475, 566, 597, 958, 1020, 1041, and  $1086\text{ cm}^{-1}$  [72].

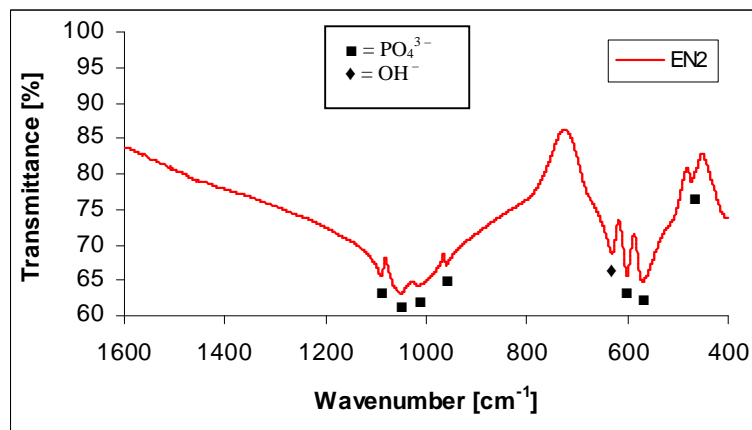
Figure 18 shows the infrared spectrum of the material prepared on experiment EN1, where is possible to identify the presence of the phosphate and hydroxyl groups, as well as the presence of a  $\text{CO}_3^{2-}$  band around  $680\text{ cm}^{-1}$ . This band can be related with the presence of CaO, which was identified on the XRD pattern of EN1, as CaO derives from  $\text{Ca}(\text{OH})_2$ , which subsequently can be transformed into  $\text{CaCO}_3$  by reacting with the atmospheric  $\text{CO}_2$  [74]. It is not possible to identify the presence of CaO in FTIR

analyses of HA samples because the band characteristic of this compound occurs at wavelengths between  $460\text{ cm}^{-1}$  and  $470\text{ cm}^{-1}$  which is absorbed by the phosphate band that coincides with those values [82, 83].



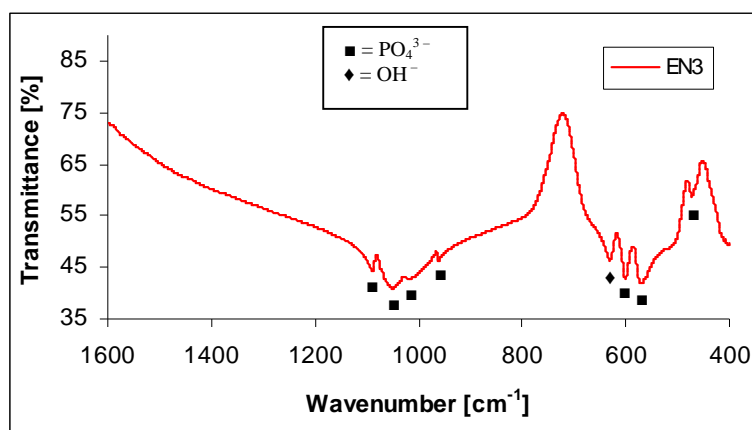
**Figure 18** – FTIR results of EN1.

The FTIR spectrum of EN2 is shown in Figure 19 presenting the phosphate and hydroxyl bands, as listed before, characteristic of the HA phase. This result is in accordance with the XRD results for this sample as no secondary phases were detected.



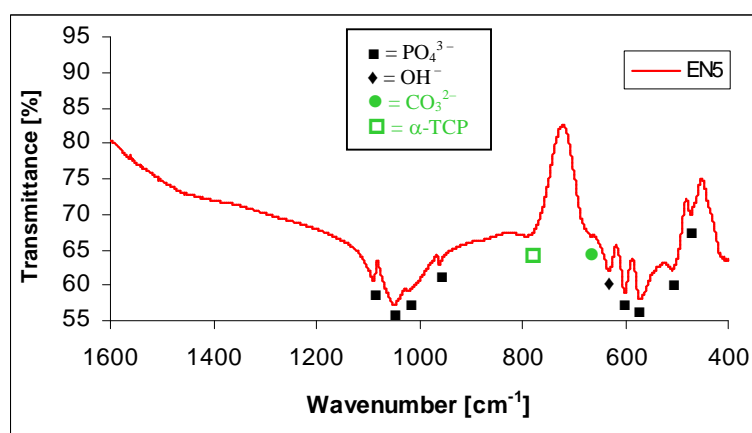
**Figure 19** – FTIR spectrum of EN2.

The results obtained with FTIR analyses of samples EN3 (Figure 20) and EN4 (data not shown) are also in accordance with the XRD results presenting the phosphate and hydroxyl bands characteristic of the HA phase.



**Figure 20** – FTIR spectrum of EN3.

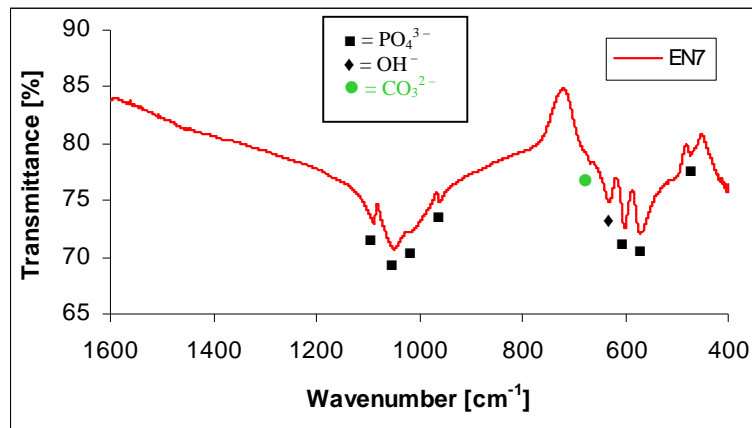
In Figure 21, besides the presence of the HA characteristic bands, there is a band at  $680\text{ cm}^{-1}$  normally related to the presence of  $\text{CO}_3^{2-}$  and a band around  $750\text{ cm}^{-1}$  defined by Queiroz *et al* [72] as a band related to the presence of  $\alpha$ -TCP. The XRD pattern of EN5 revealed the presence of  $\alpha$ -TCP and CaO. Considering the relation of CaO and  $\text{CO}_3^{2-}$ , both analyses are in accordance.



**Figure 21** – FTIR spectrum of EN5.

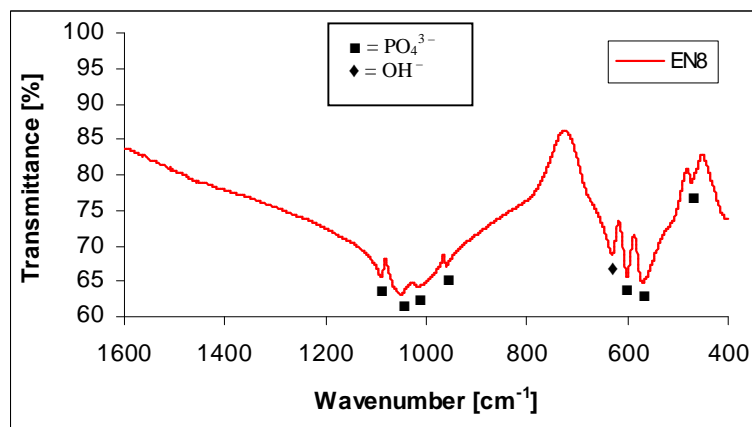
The FTIR spectrum of sample EN6 (data not shown) just showed the presence of phosphate and hydroxyl groups, according with the HA characteristic groups, as it was verified in the respective XRD pattern.

Figure 22, which corresponds to the FTIR spectrum of EN7, shows a carbonate band at  $680\text{ cm}^{-1}$  in addition to the phosphate and hydroxyl bands. The XRD pattern of this sample had shown the presence of CaO, which can be related with the appearance of the carbonate group in the FTIR analysis, as referred above.



**Figure 22** – FTIR spectrum of EN7.

Figure 23 shows the FTIR spectra of the samples EN8 presenting the phosphate and hydroxyl bands as listed before. The XRD pattern of EN8 shows the presence of  $\alpha$ -TCP, although it was not identified by FTIR probably due to its very low content.



**Figure 23** – FTIR spectrum of EN8.

FTIR spectra of samples EN9 (data not shown) and EN10 (Figure 24) are in accordance with the results obtained by the respective XRD analyses showing the presence of the groups  $\text{PO}_4^{3-}$  and  $\text{OH}^-$ , characteristic of the HA phase.

Figure 25, which corresponds to the FTIR spectrum of EN11, related to the preparation of 600g of HA, shows a carbonate band at  $680\text{ cm}^{-1}$  in addition to the phosphate and hydroxyl bands. The XRD pattern of this sample had shown the presence of CaO which can be once again related with the appearance of the carbonate group in the FTIR analysis.

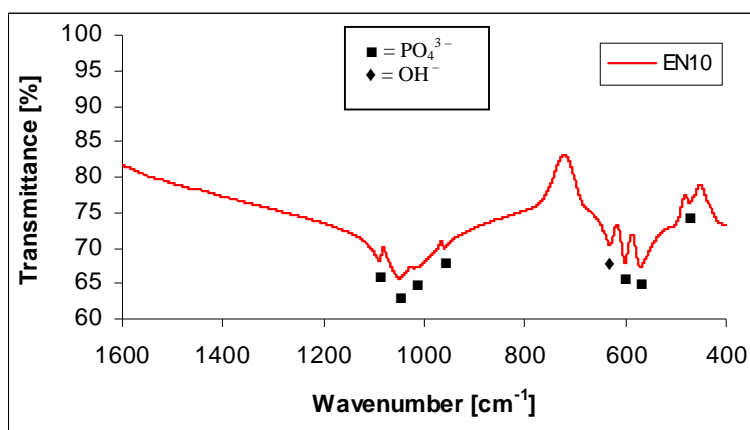


**Figure 24** – FTIR spectrum of EN10.

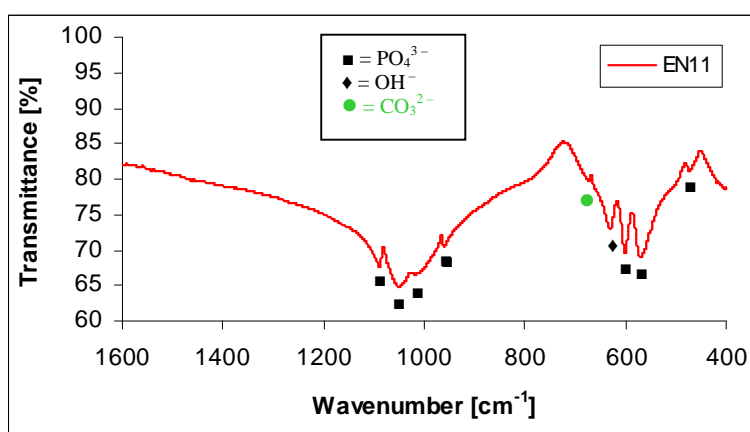


**Figure 25** – FTIR spectrum of EN11.

#### D – Ca/P and heavy metals determination

The Ca/P ratio and the concentration of heavy metals (As, Cd, Pb and Hg) were determined for the samples EN9 and EN10. These parameters are in accordance to the directive ISO 13779 [55] and are illustrated in Table 6.

**Table 6** – Ca/P ratio and metals concentration of the experiments EN9 and EN10.

Sample	Ca/P	As (mg/kg)	Cd (mg/kg)	Pb (mg/kg)	Hg (mg/kg)
EN9	1.68	<1	0.17 ± 0.03	< 0.5	< 0.5
EN10	1.69	<1	0.20 ± 0.03	< 0.5	< 0.5

#### E – HA reproducibility

The results obtained for the samples EN9 and EN10 were in accordance with the objective of this work, so a new set of 23 experiments was carried out in order to verify the consistence of the bioreactor and the reproducibility of the HA characteristics, that will allow for the certification of the HA prepared, for its use in medical applications.

This set of experiments was carried out with the same conditions of EN9 and EN10 and were quality and quantity analysed to determine the phase percentage on each sample, the Ca/P ratio, the presence of specific elements and the concentration of heavy metals. The results obtained from XRD analysis are presented in Table 7, which were calculated by the CTCV laboratory.

**Table 7** – Phase composition of each sample based on XRD analysis.

<b>Sample</b>	<b>HA (%)</b>	<b><math>\alpha</math>-TCP (%)</b>	<b>B-TCP (%)</b>	<b>CaO (%)</b>	<b>TTCP (%)</b>
<b>HA01</b>	98.76	1.24	0	0	0
<b>HA02</b>	99.47	0.53	0	0	0
<b>HA03</b>	98.06	1.61	0	0.33	0
<b>HA04</b>	97.02	0	0	2.98	0
<b>HA05</b>	96.99	1.35	0	1.66	0
<b>HA06</b>	98.80	0.76	0	0.44	0
<b>HA07</b>	98.39	0.93	0	0.68	0
<b>HA08</b>	97.08	0.62	0	2.32	0
<b>HA09</b>	98.29	0.35	0	1.36	0
<b>HA10</b>	98.73	1.27	0	0	0
<b>HA11</b>	98.87	0.70	0	0.43	0
<b>HA12</b>	98.15	0	0	1.85	0
<b>HA13</b>	99.72	0	0	0.28	0
<b>HA14</b>	97.79	1.74	0	0.47	0
<b>HA15</b>	100	0	0	0	0
<b>HA16</b>	100	0	0	0	0
<b>HA17</b>	100	0	0	0	0
<b>HA18</b>	100	0	0	0	0
<b>HA19</b>	99	<1 (lq)	<1 (lq)	<1 (lq)	<1 (lq)
<b>HA20</b>	99	<1 (lq)	<1 (lq)	<1 (lq)	<1 (lq)
<b>HA21</b>	98	1.9	<1 (lq)	<1 (lq)	<1 (lq)
<b>HA22</b>	100	<1 (lq)	<1 (lq)	<1 (lq)	<1 (lq)
<b>HA23</b>	99	<1 (lq)	<1 (lq)	<1 (lq)	<1 (lq)

The results obtained are in accordance with ISO 13779, in average the material prepared have  $98.744\% \pm 0.977$  HA phase. According to ISO 13779, the minimum content of crystalline HA should be 95% [55].

Table 8 shows the values obtained for the Ca/P ratio presenting an average of  $1.691\% \pm 0.011$ . These values are inside the range accepted by ISO 13779 which

determines that the calcium to phosphorus ratio, Ca/P, should have a value of  $1.65 \leq \text{Ca/P} \leq 1.82$  [55].

**Table 8** – Ca/P ratio based on quantity analysis (XRF).

<b>Sample</b>	<b>Ca/P (Molar Ratio)</b>
<b>HA01</b>	1.68
<b>HA02</b>	1.68
<b>HA03</b>	1.68
<b>HA04</b>	1.72
<b>HA05</b>	1.69
<b>HA06</b>	1.69
<b>HA07</b>	1.69
<b>HA08</b>	1.70
<b>HA09</b>	1.68
<b>HA10</b>	1.68
<b>HA11</b>	1.69
<b>HA12</b>	1.71
<b>HA13</b>	1.70
<b>HA14</b>	1.71
<b>HA15</b>	1.68
<b>HA16</b>	1.68
<b>HA17</b>	1.69
<b>HA18</b>	1.68
<b>HA19</b>	1.69
<b>HA20</b>	1.69
<b>HA21</b>	1.69
<b>HA22</b>	1.70
<b>HA23</b>	1.69

Analysing more specifically the presence of elements in each sample using XRF, is possible to note that the more important are P, Ca and O (Table 9). Some trace elements are found, caused by contaminations during the process, with no interference in the final phase purity of the prepared HA.

**Table 9** – Presence of elements on samples based on quality analysis (XRF).

<b>Sample</b>	<b>More Important</b>	<b>Trace Elements</b>
<b>HA01</b>	P; Ca; O	Si; Ni
<b>HA02</b>	P; Ca; O	Si
<b>HA03</b>	P; Ca; O	Si; Ni
<b>HA04</b>	P; Ca; O	Si; Mg; Ni
<b>HA05</b>	P; Ca; O	Fe; S; Si; Al; Na
<b>HA06</b>	P; Ca; O	S; Si; Al; Na; Pb
<b>HA07</b>	P; Ca; O	Si

<b>HA08</b>	P; Ca; O	Si; Al; Mg
<b>HA09</b>	P; Ca; O	Si
<b>HA10</b>	P; Ca; O	Si; Na
<b>HA11</b>	P; Ca; O	Si; Na
<b>HA12</b>	P; Ca; O	Si; Na
<b>HA13</b>	P; Ca; O	Si; Mg; Al
<b>HA14</b>	P; Ca; O	Si; Al; S; Na
<b>HA15</b>	P; Ca; O	Si; Al
<b>HA16</b>	P; Ca; O	Si; Al
<b>HA17</b>	P; Ca; O	Si; Al
<b>HA18</b>	P; Ca; O	Si; Al; S
<b>HA19</b>	P; Ca; O	Si; S
<b>HA20</b>	P; Ca; O	Si; S; Al
<b>HA21</b>	P; Ca; O	Si; S; Al; Cl; Na; Mg
<b>HA22</b>	P; Ca; O	Si; S; Al; Na; Mg
<b>HA23</b>	P; Ca; O	Si; Al; S

The presence of heavy metals was also measured by AAS for each sample (Table 10) presenting values that are inside the range of values accepted by ISO 13779.

**Table 10** – Quantity of heavy metals measured for each sample.

<b>Sample</b>	<b>AS (ppm)</b>	<b>Cd (ppm)</b>	<b>Hg (ppm)</b>	<b>Pb (ppm)</b>
<b>HA01</b>	< 1	0.09	< 0.5	1.1
<b>HA02</b>	< 1	0.11	< 0.5	< 0.5
<b>HA03</b>	< 1	0.10	< 0.5	0.5
<b>HA04</b>	< 1	0.12	< 0.5	< 0.5
<b>HA05</b>	< 1	0.11	< 0.5	0.7
<b>HA06</b>	< 1	0.11	< 0.5	0.8
<b>HA07</b>	< 1	0.14	< 0.5	< 0.5
<b>HA08</b>	< 1	0.12	<0.5	<0.5
<b>HA09</b>	< 1	<0.1	<0.5	0.6
<b>HA10</b>	< 1	0.20	<0.5	<0.5
<b>HA11</b>	< 1	0.17	<0.5	<0.5
<b>HA12</b>	< 1	0.11	<0.5	<0.5
<b>HA13</b>	< 1	0.12	<0.5	<0.5
<b>HA14</b>	<2	<0.2	<1	<1
<b>HA15</b>	<2	<0.2	<1	<1
<b>HA16</b>	<2	<0.2	<1	<1
<b>HA17</b>	<2	<0.2	<1	<1
<b>HA18</b>	<2	<0.2	<1	<1
<b>HA19</b>	< 1	<0.1	<0.5	<0.5
<b>HA20</b>	< 1	<0.1	<0.5	<0.5
<b>HA21</b>	< 1	<0.1	<0.5	<0.5
<b>HA22</b>	< 1	<0.1	<0.5	<0.5
<b>HA23</b>	< 1	<0.1	<0.5	<0.5

The maximum allowable limit fixed by ISO 13779 for metals having adverse biological reactions is a total of 50 mg/kg distributed to Arsenic (3 mg/kg), Cadmium (5 mg/kg), Mercury (5 mg/kg) and Lead (30 mg/kg) [55].

The results obtained for all analysis made with the samples prepared are in accordance with ISO 13779 for the use of HA in medical applications.

## **DISCUSSION AND CONCLUSIONS**

## DISCUSSION

The aim of this project was to develop a bioreactor that would allow for the preparation of 500g of phase pure HA in less than 5 hours of reaction time. The mentors of the present work have been well succeeded in preparing small quantities of HA using the wet method. Therefore the aim of this project is to develop a new pilot installation to allow the preparation of large quantities of HA in a reasonable period of time. The desired reaction time was fixed in five hours because on that time it is possible to do all the process in order to prepare 500g of HA in one day (eight working hours). The first step was to select, design, acquire and construct the entire unit, after which, several HA batches were prepared at different conditions. Through the physical-chemical analysis performed to the prepared HA samples in this system it was possible to confirm that the design was suitable for the purposed objective.

Analysing the XRD patterns it was possible to evaluate the presence of secondary phases illustrated by the appearance of peaks with a diffraction angle at  $30.9^\circ$  for  $\alpha$ -TCP and  $37.7^\circ$  for CaO; the most important peak of HA is exposed at  $32^\circ$ . FTIR spectra of HA samples revealed peaks of the functional groups  $\text{OH}^-$  and  $\text{PO}_4^{3-}$ , characteristic of HA presence, whose wavelengths are in accordance with literature [25, 72, 81, 82, 83]. The carbonate band  $\text{CO}_3^{2-}$  was also detected in some samples related to the presence of CaO, as well as a band related to the presence of  $\alpha$ -TCP. Other analyses were performed to determinate the Ca/P ratio, the presence of heavy metals and the presence of elements.

Botelho C.M. *et al* [25] prepared HA using the wet precipitation method with the same precursor reagents in smaller quantities, obtaining phase pure HA. This result was used as an important reference for the present research.

Several studies [48, 74, 75, 76, 77] have demonstrated the difficulties in obtaining phase pure HA when using the wet method. Santos M.H. *et al* [76] prepared HA via aqueous precipitation reaction by three synthetic routes with different experimental conditions. One of the routes utilized the same precursor reagents as the present work, showing the presence of CaO. The results obtained for the experiments using different precursor reagents ( $\text{Ca}(\text{OH})_2$  with  $(\text{NH}_4)_2\text{HPO}_4$  and  $\text{Ca}(\text{OH})_2$  with  $\text{Ca}(\text{H}_2\text{PO}_4)_2 \cdot \text{H}_2\text{O}$ ) showed the presence of CaO and also  $\beta$ -TCP. Kweh S.W. *et al* [77] found TCP and CaO preparing HA powders by the wet method using the precursor

reagents  $\text{Ca(OH)}_2$  with  $\text{H}_3\text{PO}_4$  and the same happened using  $\text{Ca(NO}_3)_2$  with  $(\text{NH}_4)_2\text{HPO}_4$ . Macipe A. L. *et al* [48] obtained large quantities of  $\beta$ -TCP using the wet method by forced hydrolysis of mixtures of calcium and phosphate salts at a high pH and temperature.

Han J.K. *et al* [60] synthesized nano-sized HA by microwave-hydrothermal method using the  $\text{Ca(OH)}_2$  mixed with  $\text{H}_3\text{PO}_4$  in deionised water and achieved a total HA purity of 99.9995%. This result was obtained for the preparation of less than 1 g of HA with a reaction time of 30 minutes which demonstrates that this method is suitable for preparation of small quantities of nano-sized HA but is not appropriated for the preparation of amounts around 500 g as experimented in the present work, because the time needed to prepare this quantity would be too long and the costs associated would be too high when compared to the method used in the present work.

The method chosen for this study, which was tested before by this research team in a very small scale and rudimental installation in the laboratory, is referenced in literature as a method that allows for the preparation of a high quality biomaterial using a preparation system with practically complete automation. The time spent for the preparation of large amounts is acceptable, allowing a competitive cost in the market.

Analysing the results obtained for the experiments performed, the experiment EN0 was carried out to obtain information regarding the pH evolution over the reaction time. The pH curve obtained showed that the pH of the reaction began near pH=12 and decreases slowly with the addition of acid until it reached the point of equivalence, which occurs around 2/3 of the total reaction time. XRD analysis of the resulting material revealed the presence of HA (69%),  $\alpha$ -TCP (24%) and  $\beta$ -TCP (7%). This means that without addition of ammonia the formation of secondary phases is favoured, which is in accordance with the literature. The literature states that it is essential to maintain the pH level above 10.5 since it allows the reaction to maintain a correct stoichiometric ratio, avoiding the formation of secondary phases [3, 87].

Analysing the Eh-pH diagram of the system Ca-P- $\text{H}_2\text{O}$  showed in Figure 26, is possible to confirm that the pH range where the HA is more stable is located between 9 and 12 [88]. Below these values is favoured the formation of secondary phases  $\alpha$ -TCP and  $\beta$ -TCP related with the appearance of  $\text{Ca}_3(\text{PO}_4)_2$  and  $\text{Ca}_2\text{P}_2\text{O}_7$ . When the pH values exceed 12, the same diagram indicates the formation of  $\text{Ca(OH)}_2$  that can derive to CaO by losing one molecule of  $\text{H}_2\text{O}$ [88].

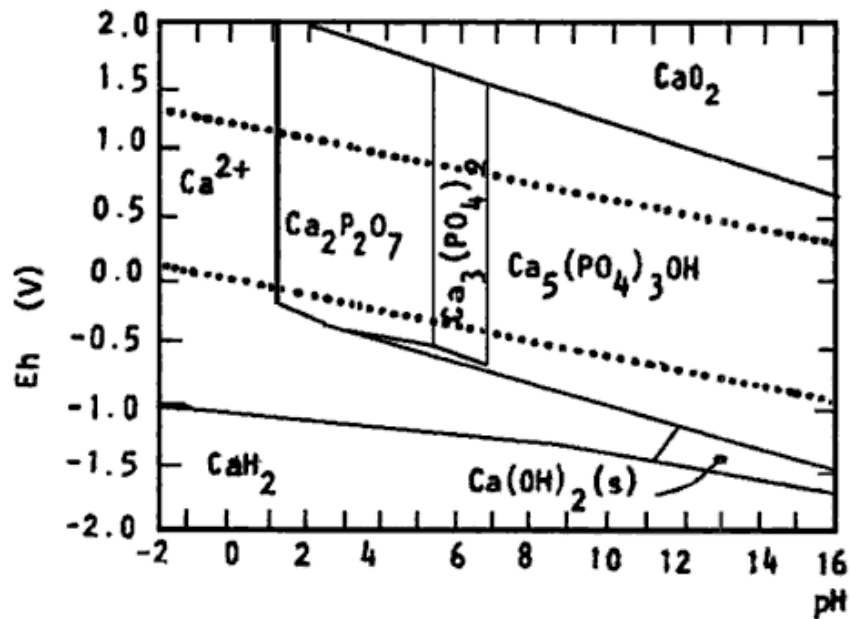


**Figure 26** – Eh - pH diagram of the Ca-P-H<sub>2</sub>O system at 25°C for 1.67 molal activity of Ca and  $a_{Ca}=1.67a_p$  [88].

The same was confirmed by EN0; if the ammonia is not added the pH decreases and the molecules of acid start to be in excess in the solution, causing the formation of calcium deficient HA [3, 85, 86, 87].

The experiments EN1 and EN2 were prepared using the same reaction conditions except the addition of H<sub>3</sub>PO<sub>4</sub> that was 8.3 ml/min in EN1 and 11.1 ml/min in EN2. It was found that using the automatic system to add ammonia, it was necessary to add 120ml in EN1 and 60ml in EN2. The XRD pattern of EN1 presents a small peak at 37.7° corresponding to the presence of CaO, while the pattern of EN2 revealed only the HA phase. The addition rate of H<sub>3</sub>PO<sub>4</sub> could be an unfavourable condition for EN2 because the fast addition of acid can lead to the creation of saturated reaction zones, without free calcium molecules to react, causing the formation of calcium deficient HA. However, EN2 results were better than those of EN1 suggesting that the addition rate used in EN2 is more appropriated for the reaction equilibrium than in EN1. The appearance of CaO on EN1 may be related to a slow acid addition rate causing an excess of calcium molecules in the solution, or with the excess of ammonia added, resulting in a pH increasing to high alkaline values, which avoids the total reaction of the calcium ions that oxidizes to CaO during sintering [3].

In order to prepare 200g of HA the quantity of reagents was doubled, maintaining all the settings of EN2, such as the acid addition rate and stir speed. In the XRD analyses of EN3 and EN4 it is not possible to observe the presence of secondary phases and the HA phase content calculated was 100%. The obtained material for both samples was phase pure HA even when the addition rate of  $\text{H}_3\text{PO}_4$  was increased from 11.1 ml/min in EN3 to 15.5 ml/min in EN4, meaning that both addition rates are suitable to be used with these reaction conditions. This result is in line with the expected since increasing the reagent quantities, increases the number of molecules free to react, allowing a higher acid addition rate, subject to an adequate agitation.

The preparation of 300g of HA in the sample EN5 was performed by using an addition rate of 15.5 ml/min. The amount of ammonia added on that experiment was 450 ml, which is a much higher amount in comparison to the 60 ml added on EN2 and the 120 ml added on EN3 and EN4. The XRD pattern of EN5 shows the presence of the secondary phases  $\alpha$ -TCP and CaO, resulting on a material with 96.5% HA phase. The presence of the secondary phase  $\alpha$ -TCP is normally related to a high acid addition rate causing the formation of calcium deficient HA [85, 86, 87]. However in this case the acid addition rate applied was the same as in EN4 and that sample was phase pure HA, the main difference was the amount of ammonia added on sample EN5, which caused the formation of CaO, as it happened in EN1, therefore some calcium ions did not react to form HA, resulting in the formation of calcium deficient HA, justifying the presence of  $\alpha$ -TCP in the XRD pattern [50, 85, 86, 87].

It is possible that a failure in the pH control system may have caused this increase on ammonia addition that takes the system out of equilibrium, a problem also verified in EN1. In order to verify if maintaining the same condition but adding manually the ammonia the problem was solved, EN6 experiment was carried out with the same reaction conditions of EN5 but adding the ammonia manually and at once. The manual addition of ammonia was maintained for all the experiments performed after EN6. The time and amount of ammonia needed, to maintain the pH above 10.5 was defined by the information given by the experiment EN0, additionally the ratio amount of ammonia added to quantity of HA prepared was optimized. The value of ammonia in millilitres was found to be around 65% of the quantity of HA to be prepared in grams.

EN6 was performed adding only 200 ml of ammonia and the material obtained was 100% HA, confirmed by the XRD pattern that shows only the presence of HA phase.

Similar conditions were applied to prepare 400g of HA in EN7, although the quantity of  $\text{NH}_3$  was increased to 300 ml following the optimization performed earlier. The XRD pattern shows the presence of CaO, that can be related with a low acid addition rate, and the HA phase present was 98.5%; therefore it was decided to double the addition rate. The result was a material with 97.9% of a HA and 2.1% of  $\alpha$ -TCP (EN8). This result indicates that this addition rate was too high; therefore new reaction regions had to be created in order to increase the number of molecules reacting at the same time.

In order to create those reaction regions and to improve the purity of the final product, a diffuser system developed during this project and it was implemented to add the  $\text{H}_3\text{PO}_4$ , which allowed a fast addition rate up to 31 ml/min. The system was tested on the following experiments, EN9 and EN10, on which 500g batches were prepared showing XRD patterns of phase pure HA. The use of the diffuser permits free molecules to react allowing a complete reaction, even with a higher addition rate, allowing the preparation of 500g of HA in approximately 5 hours that is the aim of the present project.

The Ca/P ratio measured by XRF for the experiments EN9 and EN10 showed values close to the stoichiometric HA (1.667), inside the range established by ISO 13779 (1.65 – 1.82) [55, 73].

Difficulties to obtain stoichiometric HA using the wet precipitation method are described by several studies [48, 74, 75, 76, 77]. Donadel *et al* [74] obtained values of 1.85 and 1.87 while Kweh *et al* [77] presented values higher than 1.7.

EN9 and EN10 samples were also analysed for heavy metals concentration and it was shown that the concentration is lower than the concentration allowed by ISO 13779 [55].

An additional experiment was performed to prepare a 600g HA batch (EN11) using the same reaction conditions. XRD pattern of EN11 detected the presence of CaO, a secondary phase that had been identified when the amount of ammonia added was high in EN1 and EN5 or when the acid addition rate was low in EN7. The appearance in EN11 can not be explained by the excess of ammonia, once the quantity of ammonia added was according to the other successful experiments. As mentioned previously, the

experiment EN11 was performed to study the behaviour of the bioreactor for amounts higher than 500g and was not optimized. It is possible that the formation of CaO is related to the non optimization of the acid addition rate in this experiment, causing the creation of dead reaction zones and thus the existence of free calcium ions as mentioned in bibliography [85, 86, 87]. However, the result of EN11 was a material with 97.6% of HA phase, which is above the limit determined by ISO 13779, even considering the purity calculation error (1%). This result was obtained without optimization indicating that a phase pure HA could be achieved and the installation may allow the preparation of more than 500g of phase pure HA per batch.

Analysing the FTIR spectra of HA samples, it was possible to identify peaks of the functional groups  $\text{OH}^-$ ,  $\text{PO}_4^{3-}$  whose wavelengths are in accordance with the literature [25, 72, 81, 82, 83].

The carbonate band  $\text{CO}_3^{2-}$  was detected on the samples EN1, EN5, EN7 and EN11, for a wavelength around  $680\text{ cm}^{-1}$  related to the presence of CaO, which derives from  $\text{Ca}(\text{OH})_2$  and may subsequently transform into  $\text{CaCO}_3$  by reacting with the atmospheric  $\text{CO}_2$  [74].

It is not possible to identify the band of CaO on FTIR analyses of HA samples, because the stretching vibration of this compound occurs at wavelengths between  $460\text{ cm}^{-1}$  and  $470\text{ cm}^{-1}$  which is absorbed by the phosphate band that coincides with those values [82, 83]. The presence of  $\alpha$ -TCP was also verified on the FTIR spectrum of the sample EN5, around  $750\text{ cm}^{-1}$ .

Theoretically, the hydroxyl ion has just one vibrational stretch mode referring essentially to adsorbed water at  $3600\text{ cm}^{-1}$ , however when it is located in the HA crystal structure, another mode appears at  $633\text{ cm}^{-1}$  deriving from a rotational mode, the librational mode [83]. In the present work, hydroxyl ( $\text{OH}^-$ ) peak was detected for all the samples at  $630\text{ cm}^{-1}$  corresponding to the librational mode.

There are four vibrational modes present for free phosphate ions, all infrared active. The stretching mode  $\nu_1$  appears at  $980\text{ cm}^{-1}$ , the bending mode  $\nu_2$  appears at  $363\text{ cm}^{-1}$ , the stretching mode  $\nu_3$  appears at  $1082\text{ cm}^{-1}$  and the bending mode  $\nu_4$  appears at  $515\text{ cm}^{-1}$ . In the HA crystal structure the symmetry of the tetrahedron lowers and these vibrational bands occur at wave number values around:  $\nu_1=960\text{ cm}^{-1}$ ,  $\nu_2=475\text{ cm}^{-1}$ ,  $\nu_3=1050\text{ cm}^{-1}$  and  $\nu_4=580\text{ cm}^{-1}$  [81, 82, 83]. By the analyses made during this study, the phosphate peaks were detected on all the samples at  $475\text{ cm}^{-1}$  ( $\nu_2$ ),  $566\text{ cm}^{-1}$  and  $597$

$\text{cm}^{-1}$  ( $\nu_4$ ),  $958 \text{ cm}^{-1}$  ( $\nu_1$ ),  $1020 \text{ cm}^{-1}$ ,  $1041 \text{ cm}^{-1}$ , and  $1086 \text{ cm}^{-1}$  ( $\nu_3$ ). The appearance of the triplet constituted by the peaks  $566 \text{ cm}^{-1}$ ,  $597 \text{ cm}^{-1}$  and  $630 \text{ cm}^{-1}$  are normally related to the presence of the phase HA [63].

The carbonate ions have four vibrational modes, three of which can be observed in the infrared spectrum, the bending mode  $\nu_2$  appears at  $879 \text{ cm}^{-1}$ , the stretching mode  $\nu_3$  appears at  $1415 \text{ cm}^{-1}$  and the bending mode  $\nu_4$  appears at  $680 \text{ cm}^{-1}$  [81, 82, 83]. A carbonate band was detected to the samples EN1, EN5 and EN11 around  $680 \text{ cm}^{-1}$ , shown in Figures 18, 21 and 25, respectively. This band is related with the presence of CaO in the referred samples, proved by the XRD patterns.

Morales J.G. *et al* [2] obtained phase pure HA using a precipitation method with inert atmosphere at  $85^\circ\text{C}$  and  $\text{pH}=9$ . Nevertheless some impurities like  $\text{CO}_3^{2-}$  groups appeared in the precipitates in spite of maintaining an inert atmosphere during precipitation. The same groups were verified by Donadel *et al* [74] together with a  $\text{CO}_2$  band.

The FTIR spectrum of the sample EN5 showed in Figure 21 also revealed a band around  $750 \text{ cm}^{-1}$  defined by Queiroz *et al* [72] as a band related to the presence of  $\alpha$ -TCP which is in accordance with the XRD pattern presented in Figure 14. However, the FTIR analysis of EN8 did not show the presence of  $\alpha$ -TCP revealed by its XRD pattern probably because the quantity of  $\alpha$ -TCP present in this sample was not sufficient to be identified by the FTIR analysis, as the peak presented in the XRD pattern of EN8 has half the intensity than the one showed by the XRD pattern of EN5.

The FTIR spectra obtained by Botelho *et al* [25] showed peaks of  $\text{OH}^-$  explained by the reincorporation of this groups in HA lattice, due to the reaction of HA and  $\text{H}_2\text{O}$  present in the atmosphere, during cooling furnace cycles. The same phenomenon have been verified by other studies [47, 78, 79, 80, 81], detecting  $\text{H}_2\text{O}$  bands and  $\text{OH}^-$  peaks in FTIR spectra of HA samples sintered at  $1300^\circ\text{C}$ . Han J.K. *et al* [60] find no impurities with FTIR analysis using the microwave-hydrothermal method.

The conditions of samples EN9 and EN10 were applied in 23 experiments to verify the reproducibility of the bioreactor and to allow statistical analysis, which confirm the ability of the system for the medical certification, to produce HA for medical applications. These conditions correspond to the preparation of 500g of HA per batch that was the value used to design the reactor.

The analyses of the 23 experiments were performed in the laboratory CTCV (Centro Tecnológico da Cerâmica e do Vidro) that is a certified laboratory which will allow for the medical certification of the bioreactor to produce HA for medical applications.

The set of 23 experiments carried out with the conditions of the samples EN9 and EN10 revealed the stability and reproducibility of the system presenting an average HA phase content of  $98.744\% \pm 0.977\%$  and a Ca/P ratio of  $1.691 \pm 0.011$ .

Despite all the values of this set of experiments are safely within the values defined by the standard, it is necessary to highlight the fact that were prepared 5 lots totally pure in 23. This proves that, if the production of HA in continuous batches is needed, it will be very easy to prepare HA with 100% purity with the present bioreactor.

The levels of heavy metals presented in all the 23 samples can be considered inoffensive to the human health, once the levels detected are very low and comfortably below the maximum values fixed by ISO 13779 [55]. The importance of controlling the level of heavy metals in the samples is because they can be extremely harmful to health. When absorbed by the human body, heavy metals are deposited in bone and adipose tissue, occupying the place of noble minerals. Slowly released into the body, they can cause a number of diseases, such as muscle pain and disorders, nerve disorders, kidney disorders, developmental problems in children such as attention deficit hyperactivity disorder (ADHD) and slow learning, cardiovascular disorders including high blood pressure, anaemia, loss of memory, depression, reproductive disorders including infertility, Alzheimer's disease, headache, fibrocystic breast disease (from caffeine), premenstrual syndrome (PMS), cancer, osteoporosis, fibromyalgia, arthritis [84].

The presence of trace elements detected in the samples of HA is due to contamination occurred during production, processing and analysis. During the procedures for the samples preparation, every precaution was taken to avoid contamination, especially from contact with metal. However is not possible to avoid all sources of contamination, which is insignificant in this case, once it does not affect the final purity of the samples as the quantity presented is negligible.

The parameters that define the quality of the HA prepared by the present wet precipitation method are the agitation, acid addition rate and the quantity of ammonia added (pH control). The agitation is easily optimized by regulating the stir speed to maximize turbulence and minimize splashing effects. A low acid addition rate leads with the formation of CaO while a fast acid addition rate causes the formation of  $\alpha$ -

TCP. The exceed addition of ammonia origins the formation of CaO, while the non addition of ammonia leads to the formation of  $\alpha$ -TCP and  $\beta$ -TCP. For the preparation of 500g of phase pure HA in the presence bioreactor, the ideal conditions found by this model are the ones described in EN9 and EN10.

The protocol developed and implemented throughout this project, namely the close control of the reaction parameters, the designed reactor and diffuser, allowed the preparation of 500 g HA in less than 5 hours of reaction time and suitable for medical applications, according to ISO 13779 [55].

## CONCLUSIONS

The present installation is able to prepare 500g of HA with the characteristics established by the International Organization for Standardization (ISO) to use HA in medicine.

The XRD analysis showed that the preparation of 500g of HA results in a phase pure material using the stir speed of 70 rpm, the  $\text{H}_3\text{PO}_4$  addition ratio of 31 ml/min and the quantity of ammonia added of 350 ml. The minimum pH achieved was around 10.58 and the reaction was completed after 325 minutes. With different acid adding ratios or different quantities of ammonia added the system goes out of equilibrium and secondary phases start to appear. The appearance of CaO is related to the addition of high quantities of  $\text{NH}_3$  while the appearance of  $\alpha$ -TCP is mainly related to a high acid addition ratio.

FTIR spectra of HA revealed the functional groups of  $\text{OH}^-$  and  $\text{PO}_4^{3-}$  for all the samples analysed.

The Ca/P ratio analyzed by XRF for the samples EN9 and EN10 was between 1.68 and 1.69. These values are located inside the range established by ISO 13779, “Implants for Surgery – Hydroxyapatite” that is between 1.65 and 1.82, very close to the ideal ratio of 1.667.

The concentration of metals analyzed by AAS is lower than the maximum values established by ISO 13779.

## REFERENCES

- [1] Rubin, R., Hollinger, J., Applied Principles of Bone Tissue Engineering. In: Hollinger JO, Einhorn TA, Doll BA, Sfeir C, editors. Bone Tissue Engineering. CRC Press, 2005.
- [2] Morales, J., Burgués, J., Boix T., Fraile, J., Clemente, R., Precipitation of Stoichiometric Hydroxyapatite by a Continuous Method, Cryst. Res. Technol. 2001, 36: 15–26.
- [3] Aoki, H., Science and Medical Applications of Hydroxyapatite, JAAS, 1991, Japan.
- [4] Suchanek, W., Suda, H., Yashmina, M., Kakihana, M., Yoshimura, M., J. Mater. Res. 1995, 10: 521.
- [5] Carter, D., Giori, N., Effect of Mechanical Stresses on Tissue Differentiation in the Body Implant Bed, In the Bone-Material Interface, University of Toronto Press, 1991, Canada.
- [6] Marks, C., Hermey, D., The Structure and Development of Bone, In: Principles of Bone Biology, Academic Press, 1996.
- [7] - Netter, F., Musculoskeletal System: Anatomy, Physiology, and Metabolic Disorders, Summit, New Jersey: Ciba-Geigy Corporation, (1987).
- [8] Basic Bone Biology, International Osteoporosis Foundation, Switzerland, 2007.
- [9] Van Wynsberghe, D., Noback, C., Carola, R., Bones and Bone Tissue. In: Human Anatomy and Physiology. 3rd edition, McGraw-Hill, 2000.
- [10] Graaff, V., Kent, M., Human Anatomy, 5th Edition, WEB McGraw-Hill, 1998, USA.

- [11] Donahue, J., Siedlecki, C., Vogtler, E., Osteoblastic and Osteocytic Biology and Bone Tissue Engineering. In: Hollinger, J., Einhorn, T., Doll, B., Sfeir, C., editors. Bone Tissue Engineering. CRC Press, 2005.
- [12] Hench, L., Best S. Ceramics, Glasses, and Glass-Ceramics. In: Ratner, B., Hoffman, A., Schoen, F., Lemons, J., editors. Biomaterial Science: An Introduction to Materials in Medicine. 2<sup>nd</sup> ed: Elsevier Academic Press, 2005.
- [13] Blair, H., Zaidi, M., Schlesinger, P., Mechanisms Balancing Matrix Synthesis and Degradation. *Biochem J.*, 2002; 364:329-341.
- [14] Developmental Biology of the Skeletal System. In: Hollinger, J., Einhorn, T., Doll, B., Sfeir, C., editors. Bone Tissue Engineering. CRC Press, 2005.
- [15] Seyedin, S., Rosen, D., *Current Opinion in Cell Biology*, 1990, 914-919.
- [16] Rodan, G., *Bone*, 1992; 13:S3-S6.
- [17] Parikh, S., Bone Graft Substitutes: Past, Present, Future, *Journal of Postgraduate Medicine*, 2002, 48, 142-148.
- [18] Tanner, E., Orthopedics to Take Center Stage in Coming Decade, *Datamonitor*, Queen Mary and Westfield College, UK, 2000.
- [19] The need for bone substitutes, Tutorial from Bone Tissue Engineering Center, Carnegie Mellon University, Pittsburgh, USA.
- [20] Schlenk, R., *Advances in Fusion Biologics*, Spinal Column, Cleveland Clinic Spine Institute, 2006, USA.
- [21] Betz, R., Limitations of Autograft and Allograft: New Synthetic Solutions. *Orthopedics*, 2002, 25 (5): S561-S570.

- [22] Reddy, R., Swamy, M., The use of Hydroxyapatite as a Bone Graft Substitute in Orthopaedic Conditions, *Indian Journal of Orthopaedics*, 2005, 39, 52-54.
- [23] Baumann, B., Xenotransplantation: Prevention of Human Innate Immune Responses, Dess ETH No. 16098, 2005, Swiss.
- [24] Ratner, B., Bryant, S., Biomaterials: Where We Have Been and Where We Are Going, *Annu. Rev. Biomed. Eng.*, 2004, 6:41-75, USA.
- [25] Botelho, C., Lopes, M., Gibson, I., Best, S., Santos, J., Structural Analysis of Si-Substituted Hydroxyapatite: Zeta Potencial and X-ray Photoelectron Spectroscopy. *Journal of materials science: Materials in Medicine*, 2002:13; 1123-1127.
- [26] Bone Tissue Engineering, Tutorial from Bone Tissue Engineering Center, Carnegie Mellon University, Pittsburgh, USA.
- [27] Adapted from [cs.cmu.edu/People/tissue.html](http://cs.cmu.edu/People/tissue.html)
- [28] Kakar, S., Einhorn, T. Tissue Engineering of Bone. In: Hollinger JO, Einhorn TA, Doll BA, Sfeir C, editors. *Bone Tissue Engineering*. CRC Press, 2005.
- [29] Consensus Definition, 2nd Biomaterials Consensus Conference, 1992, UK.
- [30] Ratner, B., *Biomaterials Science*, Academic Press, 2004, USA.
- [31] Guerin P., Use of Synthetic Polymers for Biomedical Application, Pacing and Clinical Electrophysiology, Volume 6, Issue 2, Blackwell Publishing, 2008.
- [32] Biomaterials, Tutorial from Bone Tissue Engineering Center, Carnegie Mellon University, Pittsburgh, USA.
- [33] Oréfice, R., Pereira, M., Mansur, H., *Biomateriais: Fundamentos e Aplicações, Cultura Médica*, 2006, Brasil.

- [34] Davies, J., Bone Engineering, 2000 in squared Toronto.
- [35] Cho, B., et al., Effect of Calcium Sulfate-Chitosan Composite: Pellet on Bone Formation in Bone Defect. *Journal of Craniofacial Surgery*, 16(2):213-224, March 2005.
- [36] Nicolodi, L., Sjölander E., Olsson K., Biocompatible Ceramics - An Overview of Applications and Novel Materials, KTH, November , 2004.
- [37] Kim, H., Song, J., Kim, H., Bioactive Glass Nanofiber-Collagen Nanocomposite as a Novel Bone Regeneration Matrix, *Journal of Biomedical Materials Research, Part A*, Volume 79A, Issue 3, Pages 698 – 705, Wiley Periodicals, Inc., 2006.
- [38] Lieberman, J., Friedlaender, G., Bone Regeneration and Repair, Biology and Clinical Applications, Humana Press, 2005.
- [39] Hutmacher, D., et al., State of the Art and Future Directions of Scaffold-Based Bone Engineering from a Biomaterials Perspective, *J. Tissue Eng. and Regenerative Medicine* 2007; 1: 245–260.
- [40] Feldman, D., Tucker, B., In a Time of Change, Orthopaedics Sector is Marked by New Modalities, BBI Newsletter, Sept., 1998.
- [41] Li, S., et al., NuOss<sup>®</sup>, a Bone Grafting Material for Oral Surgery: A Comparative Study with BioOss<sup>®</sup>, Collagen Matrix Inc., USA, 2005.
- [42] Duarte, F., Santos, J., Afonso, A., Medical Applications of Bonelike<sup>®</sup> in Maxillofacial Surgery. *Material Science Forum*, 2004; 455-456: 370-373.
- [43] Silva, M., Lemos, A., Gibson, I., Ferreira, J., Santos, J., Porous Glass Reinforced Hydroxyapatite Materials Produced with Different Organic Additives. *Journal of Non-Crystalline Solids*, 2002; 304: 286-292.

- [44] Lopes, M., Santos, J., Monteiro, F., Knowles, J., Glass-Reinforced Hydroxyapatite: A Comprehensive Study of the Effect of Glass Composition on the Crystallography of the Composite. *J. Biomed Mater Res.*, 1998; 39: 244-251.
- [45] Queiroz, A., Santos, J., Monteiro, F., Gibson, I., Knowles, J., Adsorption and Release Studies of Sodium Ampicillin from Hydroxyapatite and Glass-Reinforced Hydroxyapatite Composites. *Biomaterials*, 2001; 22 : 1393-1400.
- [46] Arramon, P., et al., Hardened Calcium Phosphate Cement Bone Implants, Meyertons, U.S.A., 2006.
- [47] Hedges, R., van Klinken, G., A review of current approaches in the pretreatment of bone for radiocarbon dating by AMS. In Long, A., and R.S. Kra (editions), *Proceedings of the 14th International 14C Conference*. *Radiocarbon*, 34, 1992.
- [48] A. Lopez-Macipe, R. Rodriguez-Clemente, A. Hidalgo-Lopez, I. Arita, M. V. Garcia-Garduno, E. Rivera, and V. M. Castano, Wet Chemical Synthesis of Hydroxyapatite Particles from Nonstoichiometric Solutions, *Journal of Materials Synthesis and Processing*, Vol. 6, No. I. 1998.
- [49] Satoa, K., Suetsugua, Y., Tanakaa, J., Inab, S., Monmab, H., The Surface Structure of Hydroxyapatite Single Crystal and the Accumulation of Arachidic Acid *Journal of Colloid and Interface Science*, Volume 224, Issue 1, Pages 23-27, 2000.
- [50] Hench, L., Wilson, J., *An Introduction to Bioceramics*, World Scientific, 1993, Singapore.
- [51] Lewis, K., Choi, A., Chou, J., Ben-Nissan, B., *Bioceramics – The Changing Role of Ceramics and Nanoceramics in Medical Applications*, *Materials Australia Magazine*, Volume 40, No 3, May/June 2007, pp. 32-34.
- [52] Nayar, S., Sinha, M., Basu, D., Sinha, A., Synthesis and Sintering of Biomimetic Hydroxyapatite Nanoparticles for Biomedical Applications, *Journal Mater. Sci. Mater Med* (2006) 17:1063–1068.

- [53] Gross, K., Ben-Nissan, B., Sorrell C., Hydroxyapatite - Properties and Applications, AZo Journal of Materials Online, 2007.
- [54] Reddy, R., Swamy, M., Hydroxyapatite as a Bone Graft Substitute: use in Cortical and Cancellous Bone, Indian Journal of Orthopaedics, 2005, 39, 52-54.
- [55] ISO 13779-1, Implants for surgery – Hydroxyapatite, Part 1: Ceramic Hydroxyapatite, International Organization for Standardization, Switzerland, 2000.
- [56] ISO 13779-2, Implants for surgery – Hydroxyapatite, Part 2: Coatings of Hydroxyapatite, International Organization for Standardization, Switzerland, 2007.
- [57] ISO 13779-3, Implants for surgery – Hydroxyapatite, Part 3: Chemical analysis and characterization of crystallinity and phase purity, International Organization for Standardization, Switzerland, 2008.
- [58] Kweh, S., Khor, K., Cheang, P., The Production and Characterization of Hydroxyapatite (HA) Powders, Journal of Materials Processing Technology 89-90 (1999) 373-377.
- [59] Earl, J., Wood, D., Milne, S., Hydrothermal Synthesis of Hydroxyapatite, Journal of Physics: Conference Series 26 (2006) 268–271.
- [60] Han, J., et al., Synthesis of High Purity Nano-Sized Hydroxyapatite Powder by Microwave-Hydrothermal Method. Materials Chemistry and Physics 99 (2006) 235-239.
- [61] Masuda, Y., Matubara, K., Sakka, S., “Synthesis of Hydroxyapatite from Metal Alkoxides Through Sol Gel Technique”, J. Ceram. Soc., Japan, 98, 1266-77, 1990.
- [62] Weng, W., Baptista J., Alkoxide Route for Preparing Hydroxyapatite and its Coatings, Biomaterials, vol. 19, n° 1-3, pp. 125-131, 1998.

- [63] Santos, M., et al., Síntese de Hidroxiapatita pelo Método Sol-Gel Utilizando Precursores Alternativos: Nitrato de Cálcio e Ácido Fosfórico, *Eclética Química*, 30 (3), 2005, Brasil.
- [64] Layrolle, P., Ito, A., Tateishi, T., Sol-Gel Synthesis of Amorphous Calcium Phosphate and Sintering into Microporous Hydroxyapatite Bioceramics, *Journal of the American Ceramic Society*, 81 (6), 1998.
- [65] Go, Y., et al., Preparation of Hydroxyapatite Powder by Using Sol-Gel Synthesis of ACP and Heating, *Seitai Kanren Seramikkusu*, 2002, Japan.
- [66] Jarcho, M., Bolen, C., Hydroxylapatite Synthesis and Characterization in Dense Polycrystalline Form, *Journal of Materials Science*, 11, 1976, 2027-2035.
- [67] Amjad, Z., Calcium Phosphates in Biological and Industrial Systems, Chapter 1, Calcium Phosphates: Structure, Composition, Solubility, and Stability, Springer, 1998, USA.
- [68] Schmidt, D., The Engineering of Chemical Reactions, New York: Oxford University Press, 1998.
- [69] Levenspiel, O., The Chemical Reactor Omnibook, Oregon St. University Bookstores, 1993.
- [70] Masters, M. Introduction to Environmental Engineering. 2<sup>nd</sup> edition, Upper Saddle River, NJ: Prentice Hall, 1998.
- [71] Perry, H., Green, W., Perry's Chemical Engineers' Handbook, 8<sup>th</sup> edition, McGraw-Hill, 2007.
- [72] Queiroz, A., et al., Laser Surface Modification of Hydroxyapatite and Glass-Reinforced Hydroxyapatite, *Biomaterials*, 25, 2004.

- [73] Santos, J., Development of Hydroxyapatite-Glass Composites for Biomedical Applications. Faculdade de Engenharia da Universidade do Porto, 1993.
- [74] Donatel, K. et al., Hydroxyapatites Produced by Wet-Chemical Methods, J. Am. Ceram. Soc., Brazil, 2005.
- [75] Monmaturapoj, N., Nano-size Hydroxyapatite Powders Preparation by Wet-Chemical Precipitation Route, Journal of Metals, Materials and Minerals, Vol. 18, N° 1, pp. 15-20, 2008.
- [76] Santos, M.H. et al., Synthesis Control and Characterization of Hydroxyapatite Prepared by Wet Precipitation Process, Materials Research, Vol. 7, N° 4, 625-630, 2004.
- [77] Kweh, S. et al., The Production and Characterization of Hydroxyapatite (HA) Powders, Journal of Materials Processing technology, 89-90, pp. 373-377, 1999.
- [78] Oliveira, J.M. et al., Bonelike®/PLGA Hybrid Materials for Bone Regeneration: Preparation Route and Physicochemical Characterisation, Journal of Materials Science: Materials in Medicine, 2005:16; 253-259.
- [79] Ducheyne, P., Bioactive Ceramics. J., Bone Joint Surg., 1994:76; 861-4.
- [80] Gross, K.A. et al., Oxyapatite in Hydroxyapatite Coating, Journal of materials science, 1998:33; 3985-3991.
- [81] Shen, Z. et al., Dense Hydroxyapatite-Zirconia Ceramic Composites with Strength for Biological Applications, Adv. Mater., 2001:13; 214-216.
- [82] Nyquist, R., Kagel, R., Handbook of Infrared and Raman Spectra of Inorganic Compounds and Organic Salts, Volume 4, Academic Press Limited, 1997, USA.
- [83] Otero, J., Ablación Láser de Blancos de Hidroxilapatita y Cerámicas Bioactivas, PhD Thesis, University of Vigo, Spain, 1999.

[84] Santos, J., Development of Hydroxyapatite Glass Composites for Biomedical Applications, PhD Thesis, University of Oporto, Portugal, 1993.

[85] Lynn, A., Bonfield, W., A Novel Method for the Simultaneous, Titrant-Free Control of pH and Calcium Phosphate Mass Yield, *Acc. Chem. Res.*, 2005, 38 (3), pp 202–207.

[86] Lynn, A., et al., Composition-controlled Nanocomposites of Apatite and Collagen Incorporating Silicon as an Osseopromotive Agent, *Wiley Periodicals, Inc. J. Biomed. Mater. Res.*, 2005.

[87] Gouveia, D., et al., Efeito do Carbonato durante a Síntese da Hidroxiapatita, 17° CBECIMat – Congresso Brasileiro de Engenharia e Ciência dos Materiais, 15 a 19 de Novembro de 2006, Foz do Iguaçu, PR, Brasil.

[88] Byrappa, K, and Yoshimura, M., *Handbook of Hydrothermal Technology, A Technology for Crystal Growth and Materials Processing*, William Andrew Inc., 2001.